

---

Masters Theses

Student Theses and Dissertations

---

1972

## Thermal expansion of nickel and iron, and the influence of nitrogen on the lattice parameter of iron at the Curie temperature

Jinn-Wen Hwang

Follow this and additional works at: [https://scholarsmine.mst.edu/masters\\_theses](https://scholarsmine.mst.edu/masters_theses)



Part of the [Metallurgy Commons](#)

Department:

---

### Recommended Citation

Hwang, Jinn-Wen, "Thermal expansion of nickel and iron, and the influence of nitrogen on the lattice parameter of iron at the Curie temperature" (1972). *Masters Theses*. 5049.  
[https://scholarsmine.mst.edu/masters\\_theses/5049](https://scholarsmine.mst.edu/masters_theses/5049)

This thesis is brought to you by Scholars' Mine, a service of the Missouri S&T Library and Learning Resources. This work is protected by U. S. Copyright Law. Unauthorized use including reproduction for redistribution requires the permission of the copyright holder. For more information, please contact [scholarsmine@mst.edu](mailto:scholarsmine@mst.edu).

THERMAL EXPANSION OF NICKEL AND IRON, AND THE INFLUENCE  
OF NITROGEN ON THE LATTICE PARAMETER OF IRON  
AT THE CURIE TEMPERATURE

BY

JINN-WEN HWANG, 1946-

A THESIS

Presented to the faculty of the Graduate School of the

UNIVERSITY OF MISSOURI-ROLLA

In Partial Fulfillment of the Requirements for the

Degree of

MASTER OF SCIENCE IN METALLURGICAL ENGINEERING

1972

Approved by

J. E. Stearns - (Advisor) J. Bilal  
Charles A. Soull

T2704  
99 pages  
c. I

## ABSTRACT

By precise X-ray measurements, the lattice parameter of pure nickel (Fisher Co., reagent grade) was found to be 3.52389 Å at 25°C. At the same temperature, the lattice parameters of iron samples were found to be: 2.86621 Å, 2.86624 Å and 2.86614 Å for purities of 99.999%, 99.985% and 99.9%, respectively. By measuring high angle back reflection lines, the linear coefficients of thermal expansion of both nickel and iron were precisely determined. Both, high purity nickel and iron, exhibited anomalies in their expansion coefficients near their Curie points. This is in agreement with some of the previously reported data.

Some data in literature show no change in lattice expansivity of iron at the Curie point. In an effort to explain the disagreement, the effect of nitrogen dissolution on the lattice parameter of iron was investigated. It was found that nitrogen decreases the Curie temperature of iron and that this shift is related to its concentration in iron. At a concentration of 110 p.p.m., the expansion coefficient of iron remained almost constant between the temperatures: 730°C and 780°C. There was no effect of nitrogen on the lattice parameter of iron at room temperature and temperatures well above the Curie point of 780°C ( within error limits ).

## ACKNOWLEDGEMENT

The author wishes to express his sincere appreciation and gratitude to Dr. M. E. Straumanis, Professor Emeritus, Department of Metallurgical Engineering, and Senior Investigator at the Graduate Center for Material Research, Space Sciences Center, U.M.R., for his patient guidance and valuable assistance during this research work.

The author is also grateful to Dr. W. J. James, Professor of Chemistry, and Director, G.C.M.R. and for the financial assistance received from G.C.M.R.

Thanks are also due to his mother and Miss Nina Lui for their constant encouragement.

## TABLE OF CONTENTS

CHAPTER	PAGE
ABSTRACT . . . . .	ii
ACKNOWLEDGEMENT . . . . .	iii
LIST OF FIGURES . . . . .	vi
LIST OF TABLES . . . . .	viii

## PART I

I. INTRODUCTION AND LITERATURE REVIEW . . . . .	2
II. EXPERIMENTAL . . . . .	6
A) SAMPLE AND SAMPLE PREPARATION . . . . .	6
B) LATTICE PARAMETERS AT ROOM TEMPERATURES	6
a) Preparation of the powder sample for X-ray diffraction . . . . .	7
b) Film loading and temperature control	8
c) Film measurement . . . . .	8
d) X-ray diffraction pattern and indexing of pattern . . . . .	8
e) Lattice parameter and coefficient of thermal expansion . . . . .	10
C) THE HIGH TEMPERATURE STUDY . . . . .	13
a) High temperature X-ray camera . . . . .	13
b) Temperature calibration . . . . .	13
c) Sample preparation for high tempera- ture X-ray diffraction . . . . .	17

CHAPTER	PAGE
d) Thermal expansion of nickel . . . . .	17
III. RESULTS AND DISCUSSION. . . . .	19
PART II	
THERMAL EXPANSION OF IRON AND THE INFLUENCE OF NITRO- GEN ON THE LATTICE PARAMETER BETWEEN 25° AND 900°C., INCLUDING THE CURIE TEMPERATURE.	
IV. INTRODUCTION AND LITERATURE REVIEW. . . . .	34
V. EXPERIMENTAL. . . . .	41
A) SPECIMEN USED . . . . .	41
B) SAMPLE PREPARATION. . . . .	43
a) Nitrogen charging . . . . .	43
b) Analysis of nitrogen in iron. . . . .	45
C) EXPERIMENTAL RESULTS. . . . .	51
a) Lattice parameter at room temperature	51
b) Lattice parameter and expansion coef- ficient at elevated temperature . . . . .	53
VI. DISCUSSION. . . . .	66
VII. SUMMARY . . . . .	71
APPENDIX - DATA AND CALCULATIONS. . . . .	74
BIBLIOGRAPHY. . . . .	87
VITA. . . . .	90

## LIST OF FIGURES

FIGURE	PAGE
1. Thermal expansion of nickel at various temperatures . . . . .	5
2. Graphical indexing of a nickel asymmetric pattern shown below, obtained with copper-radiation. . . . .	9
3. Choice of the proper radiation for nickel(f.c.c.)	11
4. Temperature calibration curve for the Seemann camera . . . . .	16
5. Variation of lattice parameter with temperature for pure nickel. . . . .	20
6. Lattice parameter versus temperature of nickel	29
7. Thermal expansion coefficient versus temperature of nickel . . . . .	31
8. Lattice parameter of pure iron at high temperature (Curie point at $768^{\circ}\text{C}$ ) . . . . .	35
9. Fe-N phase diagram . . . . .	40
10. Schematic diagram of filling the tube containing of Fe with nitrogen. . . . .	44
11. Schematic diagram of the Leco gas analyzer . .	46
12. Lattice parameter and $\alpha$ of sample A, 99.999% Fe at various temperatures . . . . .	54
13. Lattice parameter and $\alpha$ of sample A, 99.999% Fe at the Curie temperature, expansion coefficient $\alpha$ - to the right . . . . .	55

FIGURE	PAGE
14. Lattice parameter and $\alpha$ of sample B, 99.985% Fe at various temperatures . . . . .	56
15. Lattice parameter and $\alpha$ of sample B, 99.985% Fe at the Curie temperature, expansion coefficient $\alpha$ - to the right . . . . .	57
16. Lattice parameter and $\alpha$ of sample C, 99.9% Fe at various temperatures. . . . .	58
17. Lattice parameter and expansion coefficient of sample C, 99.9% Fe at the Curie temperature. . . . .	59
18. Variation of thermal expansion coefficient with temperature for pure iron. . . . .	61
19. Effect of 110 p.p.m. nitrogen on the lattice parameter of pure Fe . . . . .	64
20. Effect of nitrogen on the lattice parameter of pure Fe, the thermal expansion coefficient $\alpha$ (right side) of samples D and M. . . . .	65

## LIST OF TABLES

TABLE	PAGE
I. Determination of the true sample temperature inside the high temperature camera (air inside camera) . . . . .	15
II. Precise lattice parameters of pure nickel between 15 and 50°C, reduced to 25°C by $\alpha=1.49 \times 10^{-5} \text{ } ^\circ\text{C}^{-1}$ . . . . .	21
III. Published lattice parameters of pure nickel at room temperature (without refraction correction). . . . .	22
IV. Lattice parameters <sup>(At)</sup> of nickel in the high temperature and in the precision camera. . .	23
V. Lattice parameters of nickel at various temperatures in comparison with the values of Owen & Yates <sup>(5)</sup> , Jesse <sup>(4)</sup> and Kohlhaas et al <sup>(6)</sup>	24
VI. Thermal expansion coefficients of pure nickel at various temperatures, calculated from Eq. (4), referring to $A_{25}$ . . . . .	30
VII. Lattice parameter of alpha iron at room temperature up to the year 1943 (continuation of this table see p. 52) . . . . .	36
VIII. Analysis of high purity zone-refined iron (sample B) . . . . .	42
IX. Determination of the volume of the system. .	48

TABLE	PAGE
X. Sample D, E and F, prepared from 0.4 g of sample A (99.999% Fe) charging it with various amounts of N <sub>2</sub> at 630°C for various time periods . . . . .	50
XI. Lattice parameter of pure iron determined between 1935 - 1971. . . . .	52
XII. Coefficient of linear thermal expansion of pure iron $\alpha \times 10^6$ (millionths per °C). . . . .	60
XIII. Thermal expansion coefficients of sample D, E & F above 600°C. . . . .	63
XIV. Lattice parameters of pure Fe (sample A, B & C) and of N-containing Fe (sample D, E & F), $a$ in Å of samples above 780°C. . . . .	68
XV. Lattice parameter of 99.999% pure iron (sample A) . . . . .	75
XVI. Lattice parameter of 99.985% pure iron (sample B) . . . . .	77
XVII. Lattice parameter of 99.9% pure iron (sample C) . . . . .	78
XVIII. Lattice parameter of sample D**, containing 220 p.p.m. N . . . . .	80
XIX. Lattice parameter of sample E, containing 170 p.p.m. N . . . . .	82
XX. Lattice parameter of sample F, containing 110 p.p.m. N . . . . .	83

## PART I

## THE THERMAL EXPANSION OF NICKEL

## CHAPTER I

## INTRODUCTION AND LITERATURE REVIEW

Like the compressibility and heat capacity, the thermal expansion coefficient is important because it is one of the independent thermodynamic properties which can be measured experimentally with high precision.

With the development of the theory of the defect structure of crystals, high precision measurements of lattice parameters by the X-ray method become important together with the density in the exploration of such structures. Furthermore, accurate determinations of lattice parameters enable one to investigate the thermal expansion of various crystalline substances, even if they are available only in amounts of a few milligrams.

It is generally believed that when a crystal undergoes a sudden change in its magnetic or electronic properties, i.e. with the variation of the temperature going through the Curie point, a change in thermal expansion should occur. This was shown with Cr, Co, Ni, . . . etc.

Although it is well established that nickel exhibits lattice parameter anomalies, and hence an anomalous thermal expansion when raising the temperature through the Curie point, the data reported differ substantially, as reported by various authors. It is, therefore, of interest

to recheck the lattice parameters and the thermal expansion coefficients of pure nickel at room and elevated temperatures.

Most investigators found a thermal expansion anomaly of pure nickel in the Curie temperature region. By a dilatometric method Colby<sup>(1)</sup> found that the coefficient of expansion of high purity electrolytic nickel increased rapidly between 220°C and 360°C, returning to its previous value at about 370°C. With other specimens of lower purity nickel the same effect was observed: the thermal coefficient increased with temperature until a critical region in the neighborhood of the magnetic transformation was reached, and then decreased to a certain value before increasing again with further rise of temperature.

Hidnert<sup>(2)</sup>, who determined the thermal expansion of a nickel specimen, 99.4 per cent pure, in the form of a 12 inches long rod, over the temperature range 25°C to 900°C, found an irregularity in the expansion near 350°C.

Clarke Williams<sup>(3)</sup>, using a sensitive optical method and a single crystal of nickel, made a detailed investigation of the thermal expansion of the metal near the mentioned transformation temperature. He found that the purest nickel available showed a maximum in expansivity

at about  $355^{\circ}\text{C}$  and then a sudden drop beyond this temperature.

While investigating for a new crystal form of nickel at temperatures extending from  $450^{\circ}\text{C}$  to  $1200^{\circ}\text{C}$ , Jesse<sup>(4)</sup> made X-ray measurements of very pure nickel, obtained by reducing pure nickel oxide in hydrogen. The data obtained by him are plotted versus temperature in Fig. 1.

The same was done with the results of Owen and Yates<sup>(5)</sup> who measured the thermal expansion of 99.98% pure nickel over a temperature range from  $12^{\circ}\text{C}$  to  $600^{\circ}\text{C}$  by determining the lattice parameters (Fig. 1). The maximum value of the thermal coefficient of expansion occurred at  $370^{\circ}\text{C}$ , at the point of magnetic transformation.

Kohlhaas et al.<sup>(6)</sup> determined the lattice parameters of polycrystal nickel, 99.997% pure, as a function of temperature up to melting point. There was a definite influence of the magnetostrictive region on the volume expansion (Fig. 1).

The measurements were reported with a nickel single crystal (99.977% pure) by Dünner and Kohlhaas<sup>(7)</sup> between  $90^{\circ}$  and  $1670^{\circ}\text{K}$ . The temperature dependence of the lattice parameters was found in accordance with the magnetostrictive behavior of nickel. There was a maximum of the expansion coefficient at  $630^{\circ}\text{K}$  ( $357^{\circ}\text{C}$ ).

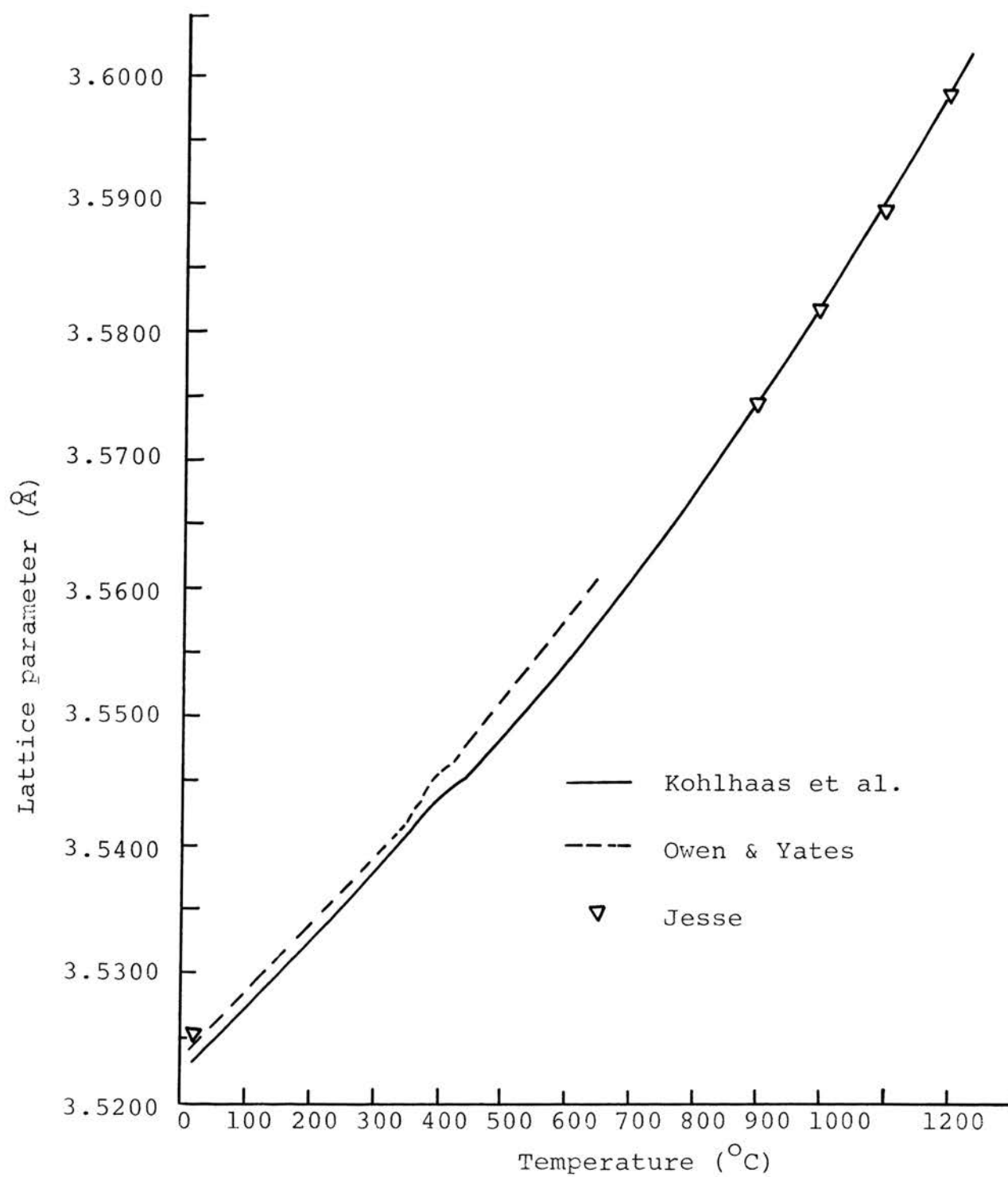


Figure 1 Thermal expansion of nickel at various temperatures.

## CHAPTER II

## EXPERIMENTAL

## A. SAMPLE AND SAMPLE PREPARATION

Pure nickel powder (below 350 mesh), low in cobalt, obtained from the Fisher Co., (catalog #N-40) was used throughout this part of investigation.

The nickel powder for the room temperature X-ray work was treated by annealing it in a stream of ultra-pure hydrogen at 600°C for 4 hours and then furnace cooled.

For high temperature work, pure nickel powder was sealed under vacuum in a 0.3mm thin-walled quartz capillary and annealed in the high temperature X-ray camera.

## B. LATTICE PARAMETERS AT ROOM TEMPERATURES

The circumference of the film exposed in a cylindrical camera can be exactly determined without knowing its diameter or the amount of film shrinkage by the asymmetric method of film loading. It is possible to calculate the lattice parameters by measuring the high-angle lines of powder patterns of a crystalline substance with high precision, provided that the thin and uniform sample was mounted carefully, centered accurately, maintained during the X-ray exposure at a constant and known temperature,

and sharp diffraction lines resulted. The equipment and the experimental method are described in the literature (8), (9), (10).

(a) Preparation of the powder sample for X-ray diffraction

To get sharp diffraction lines, well-centered and undistorted crystalline samples are necessary. A fiber of lithium-boron glass of about 0.05mm diameter was glued to the tip of the sample holder in the camera cover. The whole was then placed under a microscope in such a way that the glass fiber was horizontal. By adjusting the screws of the sample centering head under the microscope, the glass fiber was positioned until its axis of rotation coincided with the camera cover axis.

The glass fiber was then coated with a thin layer of oil which served as an adhesive. The powder was spread uniformly over the coating so that the overall diameter did not exceed 0.2mm. A thin layer of powder is necessary to prevent broadening and shifting of the diffraction lines and to avoid the error due to absorption<sup>(11)</sup>.

After mounting, the sample was centered again and the cover with the powder mount was put on the camera. By viewing the powder sample within the camera through the collimator using a magnifying glass, the centering was

checked again.

(b) Film loading and temperatures control The film was loaded asymmetrically in the powder camera (64mm diameter). The details and advantages of this technique are described in the literature<sup>(10)</sup>.

The whole camera was placed in a thermostat which maintained a constant temperature between 15 to 50°C with an accuracy of 0.05°C by circulating water. After 75 minutes exposure, all films were processed in a standard manner.

(c) Film measurement A comparator having a precision of 0.001mm was used to measure the diffraction lines on the asymmetric film (Fig. 2). The film was placed between two glass plates of the comparator and adjusted until the intersection of the cross hairs of the microscope traveled along the equator of the diffraction pattern.

By measuring the maximum density position of the line, the effective film circumference, the conversion factor (from mm to degrees) and the high back reflection Bragg angles were calculated<sup>(12)</sup>.

(d) X-ray diffraction pattern and indexing of pattern  
Applying a graphical method<sup>(13)</sup>, copper radiation

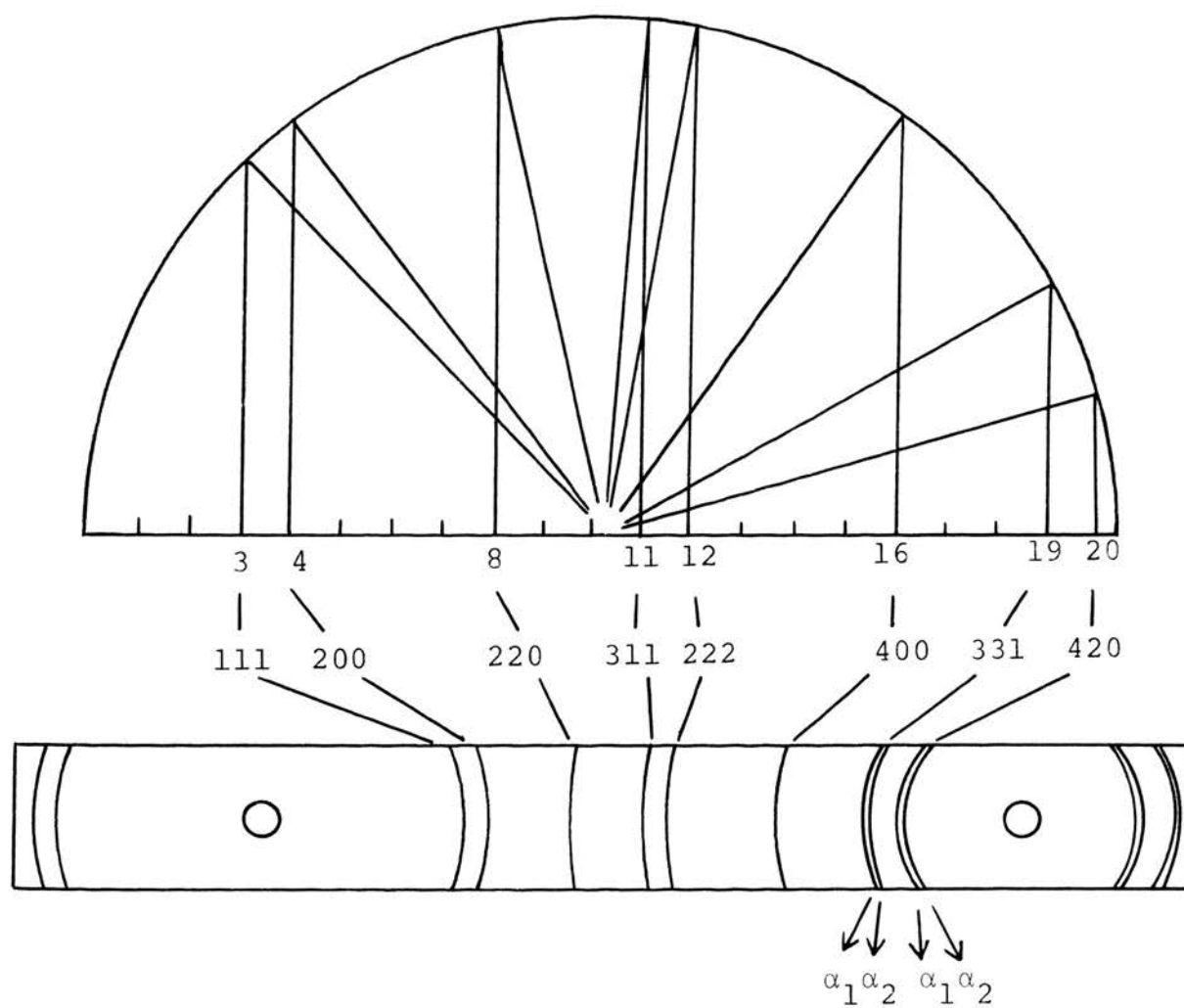


Figure 2 Graphical indexing of a nickel asymmetric pattern shown below, obtained with copper radiation.

( $\lambda K \alpha_1 = 1.54051 \overset{\circ}{\text{Å}}$ ) was found to be appropriate to get the highest back reflection lines. They also were sharp and intense (Fig. 2).

The nickel diffraction pattern obtained was also indexed graphically, using the reciprocal lattice method<sup>(13)</sup>, as shown in Fig. 3.

(e) Lattice parameters and coefficient of thermal expansion

The lattice parameters were calculated from the last indices ( $\Sigma h^2 = 20$ , i.e.  $hkl = 420$ ) using for the cubic system the formula:

$$a = \lambda ( h^2 + k^2 + l^2 )^{1/2} / 2 \sin\theta \quad (1)$$

where  $\lambda$  is the wavelength of the radiation used ( $\text{Cu K } \lambda_1 = 1.54051 \overset{\circ}{\text{Å}}$ ),  $\theta$  - the reflection (Bragg) angle and  $h, k, l$  - the Miller indices of the reflecting plane.

In equation(1), the wavelength  $\lambda$ , and the Miller indices,  $h, k$  and  $l$  are constant for a certain substance and reflection plane. Hence, Eq. (1) can be reduced to:

$$a = K / \sin\theta \quad (2)$$

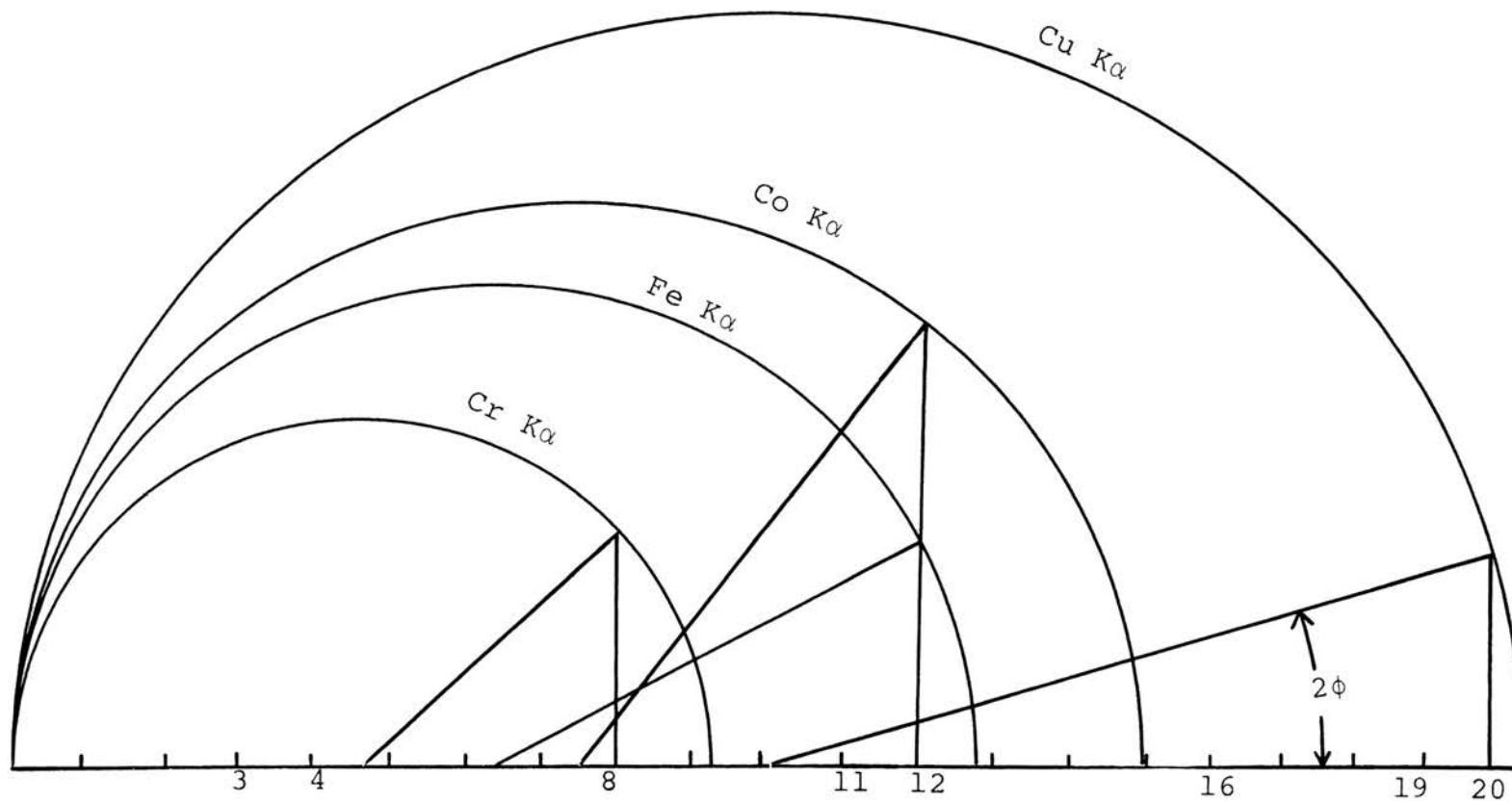


Figure 3 Choice of the proper radiation for nickel (f.c.c.).  
 (Copper radiation gives the lowest back reflection angle)

$$\text{where } K = \lambda ( h^2 + k^2 + l^2 )^{1/2} / 2 \quad (3)$$

In the present case,  $K = 3.44468508$  for the plane (420) and Cu  $K\alpha_1$  radiation.

The coefficients of thermal expansion were calculated from the average lattice parameters at different temperatures using the following equation:

$$\alpha = ( a_t - a ) / a(t - t_0) \text{ or } (da/dt)_t / a_t \quad (4)$$

where  $a_t$  is the lattice parameter at the temperature  $t$  of exposure and  $a$  is the parameter at  $t_0 = 25^\circ\text{C}$ .

In equation (4),  $(da/dt)$  is actually represented by the slope of the straight line in the plots of the lattice parameters versus various temperatures. From the expansivity and the lattice parameter at  $25^\circ\text{C}$ , the coefficients of thermal expansion were calculated.

### (C) THE HIGH TEMPERATURE STUDY

Using a high temperature camera, the thermal expansion of pure nickel powder was determined up to  $1100^{\circ}\text{C}$ .

(a) High temperature X-ray camera A high temperature circular camera, made by Dr. Seemann in Germany, was used in this investigation. This camera, which can be operated up to  $1350^{\circ}\text{C}$ , has a platinum heating coil closely surrounding the sample. The camera was originally designed for the symmetric film loading, but it was modified here for use with asymmetric films to ensure more precise lattice parameter determination. By shifting the movable cassette containing free film parallel to the cylinder axis by 5 mm, five exposures at different temperatures could be obtained on one film. The details of the camera are already described<sup>(14)</sup>.

(b) Temperature calibration The temperature inside the camera was set by an electronic controller, connected with a platinum-platinum-rhodium thermocouple, its tip being located close to the end of the powder sample inside the high temperature camera. Because of the unavoidable thermal gradients inside the camera, the thermocouple did not actually measure the true temperature of the sample, therefore, the camera had to be calibrated. However, it could

be assumed that the temperature was uniform over the portion of the sample exposed to X-rays, because of its very small size.

The temperature calibration of the high temperature camera consisted simply in establishing the relationship between the true temperature of the exposed portion of the sample and the temperature read from the indicating instrument of the electronic controller.

This can be done by recording the changes (transitions and melting) that take place in the diffraction pattern of the various metals by slowly increasing or decreasing the temperature of the sample. By preparing several diffraction photographs above and below the melting point of the metal, the temperature on the indicating instrument was fixed. The following metals were used for this purpose: In, Bi, Zn, Sb, Ag, and Au. Their melting points in  $^{\circ}\text{C}$  are 156.5, 271, 419, 630.5, 960.5 and 1063 respectively. Pure iron with  $A_3$  point at  $910^{\circ}\text{C}$  was also used for this purpose. As the metal passed from the crystalline to the liquid state, its diffraction pattern disappeared and the respective temperature on the indicating instrument was noted. The temperature readings of the indicating instrument were controlled within  $\pm 2^{\circ}\text{C}$ . The results are shown in Table I and plotted in Fig. 4.

TABLE I  
 Determination of the true sample temperature  
 inside the high temperature camera.  
 (air inside camera)

Metal	Melting point (°C)	Indicating instrument reading (°C)		
		(A)	(B)	(C)
In	156.5	125	70	133
Sn	232	175	-	-
Bi	271	-	180	242
Pb	327	265	-	-
Zn	419	-	338	383
Sb	630.5	588	580	603
Al	660	-	-	641
Fe (A <sub>3</sub> )	910	880	885	-
Ag	960.5	-	933	955
Au	1063	1041	1041	1068

(A) Present work

(B) Kim<sup>(15)</sup>

(C) Riad<sup>(14)</sup>

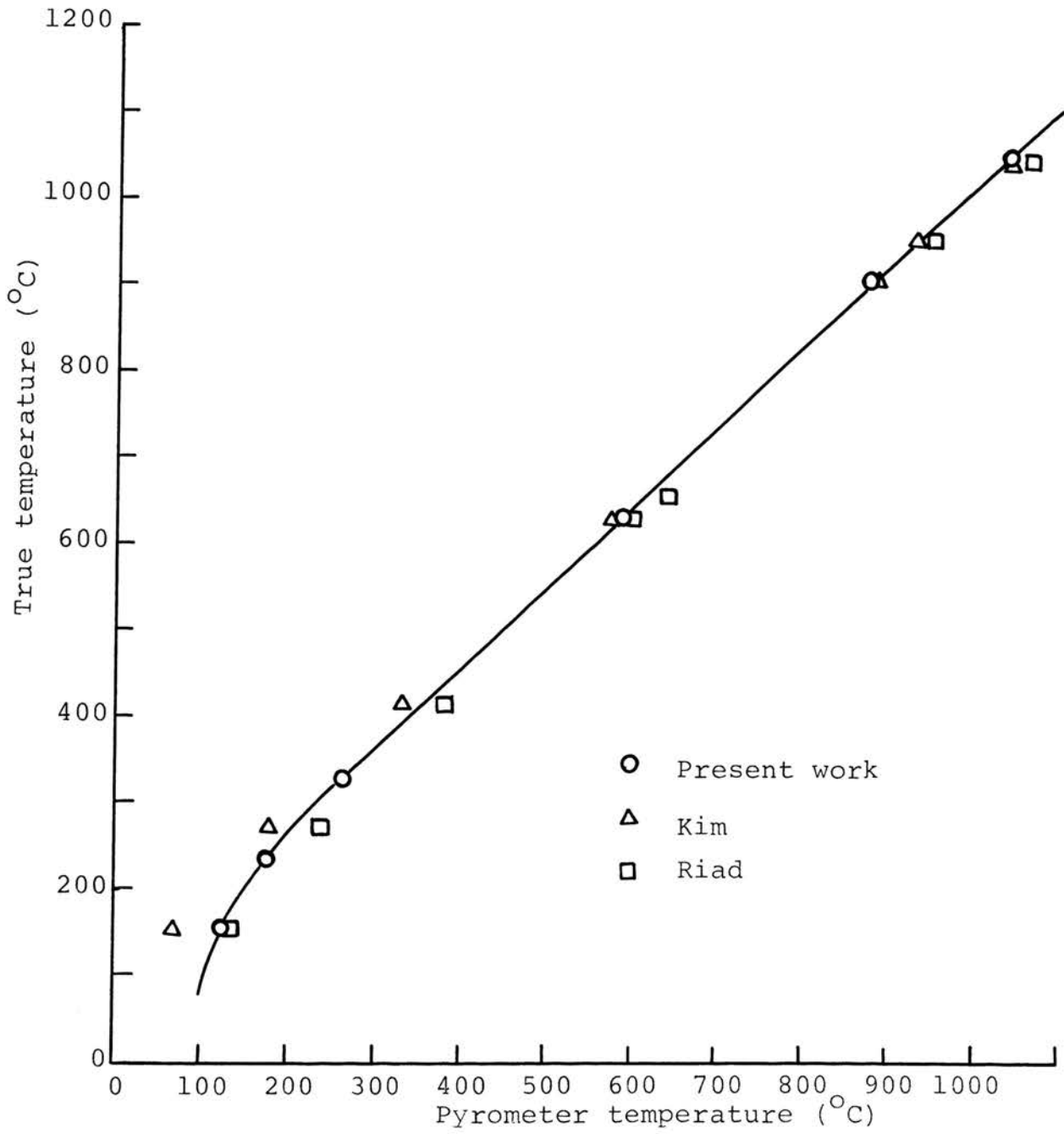


Fig. 4 Temperature calibration curve for the Seemann camera.

comparing them with previous calibration results<sup>(14,15)</sup>.

It has to be mentioned that all the X-ray exposures of the present investigation were made under the same environmental conditions as for the calibration.

(c) Sample preparation for high temperature X-ray diffraction

Pure nickel powder was placed inside a quartz capillary sealed at one end. The diameter of the capillary was smaller than 0.3mm, and the height of the powder sample was kept close to 4mm. To reduce the amount of air inside the capillary and also to increase the strength of the capillary for handling, a quartz rod (plug) was inserted inside the capillary tube and the capillary tube was sealed off under vacuum. The quartz capsule was then fused to the tip of a quartz rod of 10mm in length as a handle and the whole was cemented to the tip of the sample holder by means of MgO cement. The sample was adjusted and centered under a microscope.

(d) Thermal expansion of nickel Asymmetric X-ray diffraction patterns were obtained at various temperatures from the powder sample described above.

The lattice parameters were calculated from (420) and the Bragg angle of about  $78^{\circ}$  obtained with Cu  $K\alpha_1$

radiation in the same way as from room temperature films.

The coefficients of linear thermal expansion were calculated from:

$$\alpha = (da/dt)_t / a_{25} \quad (5)$$

where  $(da/dt)_t$  is the slope of the tangent to the expansivity curve at a certain temperature  $t$ . Reference is made to  $a_{25}$ , the lattice parameter of pure nickel at  $25^\circ\text{C}$ .

## CHAPTER III

## RESULTS AND DISCUSSION

By the technique mentioned, the errors due to shrinkage of the film, absorption of the X-ray beam by the specimen, divergence of the X-ray beam, eccentricity of the sample in the camera etc. are reduced to a minimum extent. Errors due to inaccurate knowledge of the temperature of the sample are also eliminated by keeping the whole camera at a constant and known temperature. Under such conditions, a precision of the order of 1:20,000 has been reached.

Table II shows the present lattice parameters of pure nickel at various temperatures. A straight line relationship in the temperature-lattice parameter plot is obtained and a thermal expansion coefficient of  $14.9 \times 10^{-6} \text{ } ^\circ\text{C}^{-1}$  (see Fig.5) is calculated. This is in good agreement with the value of about  $14.5 \times 10^{-6} \text{ } ^\circ\text{C}^{-1}$  given by Owen & Yates as deduced by extropolation of their  $\alpha$  vs temperature plot. With the present  $\alpha$  the lattice parameters at various temperatures are deduced to those of  $25^\circ\text{C}$  and the refraction correction is added (Table II).

The lattice parameter of the nickel sample determined in this investigation is compared with that of pure nickel of previous determinations in Table III. The present

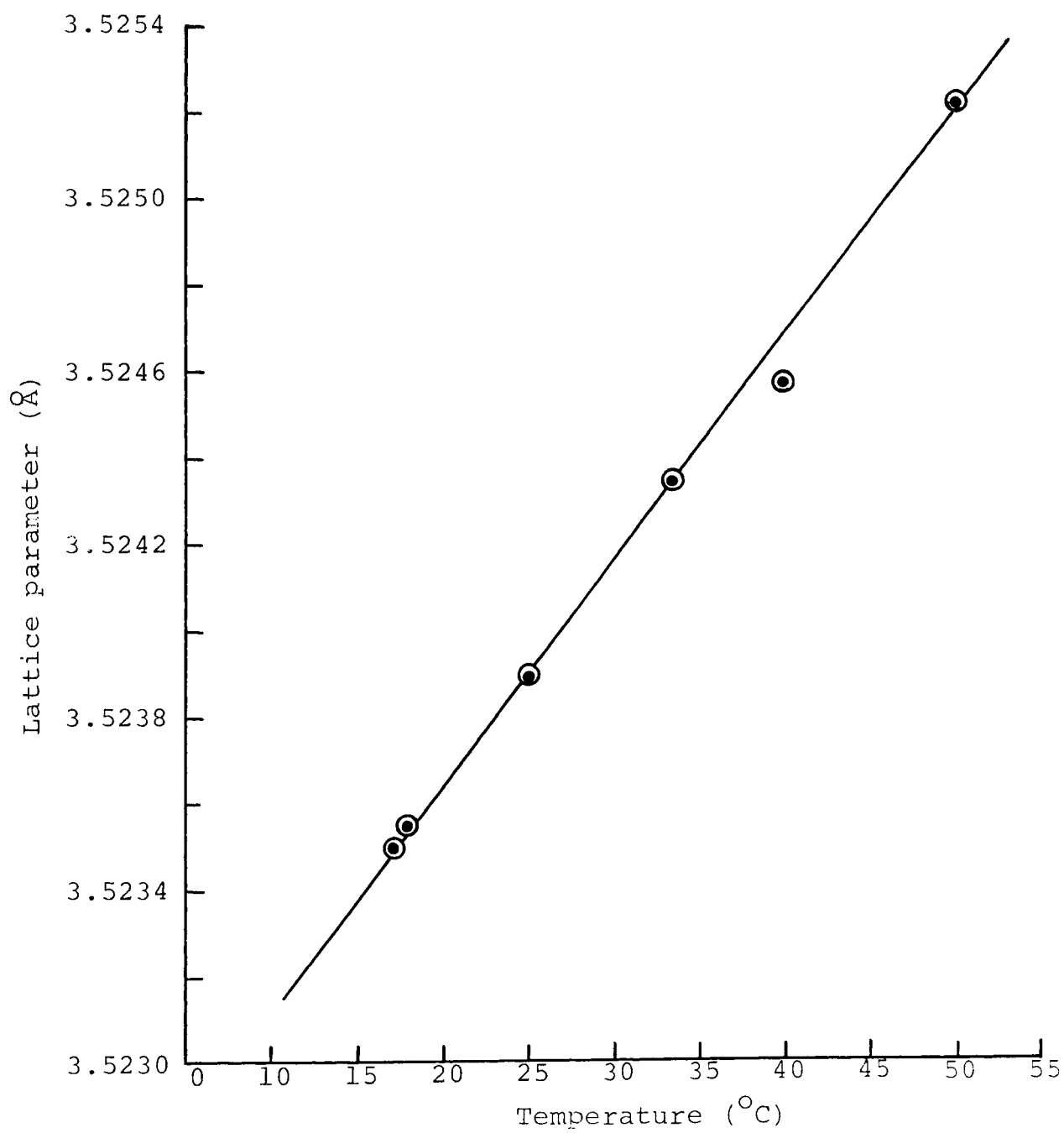


Figure 5 Variation of lattice parameter with temperature for pure nickel.

TABLE II

Precise lattice parameters of pure nickel between 15 and 50°C, and reduced to 25°C by  $\alpha = 1.49 \times 10^{-5} \text{ } ^\circ\text{C}^{-1}$ .

Temp. (°C)	$a_t$ (Å)	$a_{25}$ (Å)
17.3	3.52349	3.52389
17.8	3.52354	3.52391
25.0	3.52389	3.52389
33.4	3.52434	3.52390
40.0	3.52457	3.52378
50.0	3.52523	3.52392

Average:  $3.52388 \pm 0.00003^*$

Refr. corr. <sup>\*\*</sup> +)  $0.00011$

Final value ( $a_{25}$ ) :  $3.52399 \pm 0.00003$

\* Using the equation

$$S' = 0.675 \left\{ \frac{\sum (dx)^2}{(n-1)} \right\}^{1/2} \quad (6)$$

where  $S'$  is the probable error,  $\sum (dx)^2$  the sum of the square of the deviations, and  $n$  the number of measurements or degrees of freedom.

\*\* See reference (15), equation (8).

TABLE III  
Published lattice parameters of pure nickel at  
room temperature (without refraction correction).

Author	T(°C)	Year	a <sub>t</sub>	a <sub>25</sub> **	Remark (purity)
Jesse <sup>(4)</sup>	20	1934	3.5251	3.5253 <sub>6</sub>	trace of Co and Si
Owen and Yates (5)	18	1936	3.5243	3.5246 <sub>7</sub>	99.98% Ni
Kogan and Bulatov(16)	27 (300°K)	1962	3.5157	3.5156	99.98% Ni <sup>58</sup> Foil
Kohlhaas et al. (6)	20	1967	3.5232	3.5234 <sub>6</sub>	99.997% Ni
Present work	25.0	1971	3.52389	3.52389	purified, low in cobalt by Straumanis camera
Present work	25.7	1971	3.5239	3.5238 <sub>7</sub>	purified, low in cobalt by high temp. camera

\*\* Reduced lattice parameter from t°C to 25°C, using  
 $\alpha = 1.49 \times 10^{-5} \text{ } ^\circ\text{C}^{-1}$

$a_{25} = 3.52389 \text{ \AA}$ , obtained in the Straumanis camera, and  $a_{25} = 3.5239 \text{ \AA}$ , in the high temperature Seeman camera, are close to that reported by Kohlhaas et al.<sup>(6)</sup> and only slightly lower than that of Owen and Yates<sup>(5)</sup>. All these results are in very poor agreement with the  $a_{25}$  of Kogan and Bultatov<sup>(16)</sup> who employed high-angle X-ray pattern by a graphical method<sup>(17)</sup> and obtained a comparatively low value for a electrolytic nickel foil ( $a_{27} = 3.5157 \text{ \AA}$ ).

High temperature thermal expansion of nickel was determined in a high temperature X-ray camera, modified for placing asymmetric films. The results are collected in Table V. That this high temperature camera works as well at room temperature as a precision (Straumanis) camera is shown in Table IV.

TABLE IV  
Lattice parameters ( $a_t$ ) of nickel in the high temperature and in the precision camera

Temperature (°C)	Lattice parameters ( $\text{\AA}$ )			
	Precision camera		High temperature camera	
	$a_t$	$a_{25}^*$	$a_t$	$a_{25}^*$
25.0	3.52389	3.52389	-	-
25.7	-	-	3.5239	3.5239
40.0	3.52457	3.52378	3.5247	3.5238
50.0	3.52523	3.52392	3.5252	3.5239
Average ( $a_{25}$ ) :		3.52386		3.5238 <sub>6</sub>

\* The  $a_t$  values reduced to the same temperature by  
 $\alpha = 1.49 \times 10^{-5} \text{ }^\circ\text{C}^{-1}$ .

TABLE V

Lattice parameters of nickel at various temperatures  
in comparison with the values of Owen & Yates<sup>(5)</sup>,  
Jesse<sup>(4)</sup> and Kohlhaas et al.<sup>(6)</sup>

Film No.*	T(°C)	Lattice parameter (Å)		
		Present work	Owen & Yates	Kohlhaas et al.
	16		3.5243	
	20			3.5246
#2	25.7	3.5239		
#3	40	3.5247		
	47			3.5246
#7	50	3.5252		
	90			3.5266
	98		3.5283	
#2	115	3.5289		
	134			3.5285
	186		3.5330	3.5315
	220			3.5337
#2	225	3.5345		
#13	250	3.5359		
	257		3.5295	
#2	273	3.5370		
	282			3.5373

\* Referred to the present work

TABLE V  
(continued)

Film No.	T(°C)	Present work	Owen & Yates	Kohlhaas et al.
#12	291	3.5386		
	301		3.5390	
#12	308	3.5399		
#3	315	3.5403		
#11	325	3.5410		
#3	330	3.5412		
	333		3.5409	
#11	342	3.5421		
	345			3.5404
#13	350	3.5427		
	352		3.5422	3.5413
	359		3.5428	
#12	360	3.5433		
#11	361	3.5433		
	365		3.5433	
	367			3.5415
#12	372	3.5438		
	373		3.5439	
	378		3.5442	
#13	380	3.5442		
	382			3.5430

TABLE V  
(continued)

Film No.	T(°C)	Present work	Owen & Yates	Kohlhaas et al.
#5	389	3.5445		
	398		3.5455	
#5	399	3.5451		
	405		3.5458	
#5	407	3.5455		
	411		3.5460	
#5	416	3.5460		
#6	427	3.5466		
	429		3.5474	
#6	437	3.5472		
#6	440	3.5474		
	441			3.5450
#1	455	3.5483		
	460		3.5494	
#1	487	3.5500		
#1	505	3.5511		
	513			3.5492
#1	550	3.5537		
	557		3.5553	
	603		3.5580	
#6	631	3.5580		
	628		3.5567	

TABLE V  
(continued)

Film No.	T(°C)	Present work	Owen & Yates	Jesse
	20		3.5232	3.525±0.001
#8	703	3.5615		
	718		3.5617	
#7	745	3.5652		
	772		3.5650	
#8	787	3.5666		
#10	834	3.5700		
	851		3.5716	
	874		3.5736	
#9	877	3.5738		
	900			3.575±0.002
#10	901	3.5741		
	945		3.5798	
#9	947	3.5780		
#10	990	3.5804		
	1000			3.582±0.002
	1028		3.5852	
#8	1034	3.5848		
	1100			3.590±0.002
	1200		3.5987	3.599±0.002

---

(All lattice parameters are converted from Kx unit into Å  
using conversion factor of 1.00202)

There exists a slight thermal expansion anomaly in the region of magnetic transformation of pure nickel ( $300^{\circ}$  to  $400^{\circ}\text{C}$ ) followed by an increasing expansivity at higher temperatures. This is illustrated in Fig.6 along with results of other investigators.

The present results are in good agreement with those of Owen and Yates below  $450^{\circ}\text{C}$  and with those of Kohlhaas, et al. above  $550^{\circ}\text{C}$ . Also, the temperature of the expansion anomaly, agrees in all three cases ( within error limits ). The variations in the reported lattice parameters may be contributed to the differences in the purities of the nickel samples and the uncertainty in controlling and measuring the temperature of the sample within the camera.

The thermal expansion coefficients of nickel were obtained from the plot of lattice parameter versus temperature (see Fig.6) using Eq.(4). These are summarized in Table VI and illustrated graphically in Fig.7. The curve obtained by Owen and Yates<sup>(5)</sup> (shown by dashed lines) also included in Fig.7.

The present work indicated a maxima in the expansion curve ( See Fig.7 ) at  $330^{\circ}\text{C}$ , in fair agreement with Owen and Yates and Kohlhaas, et al. who obtained  $370^{\circ}$  and  $357^{\circ}\text{C}$ ,

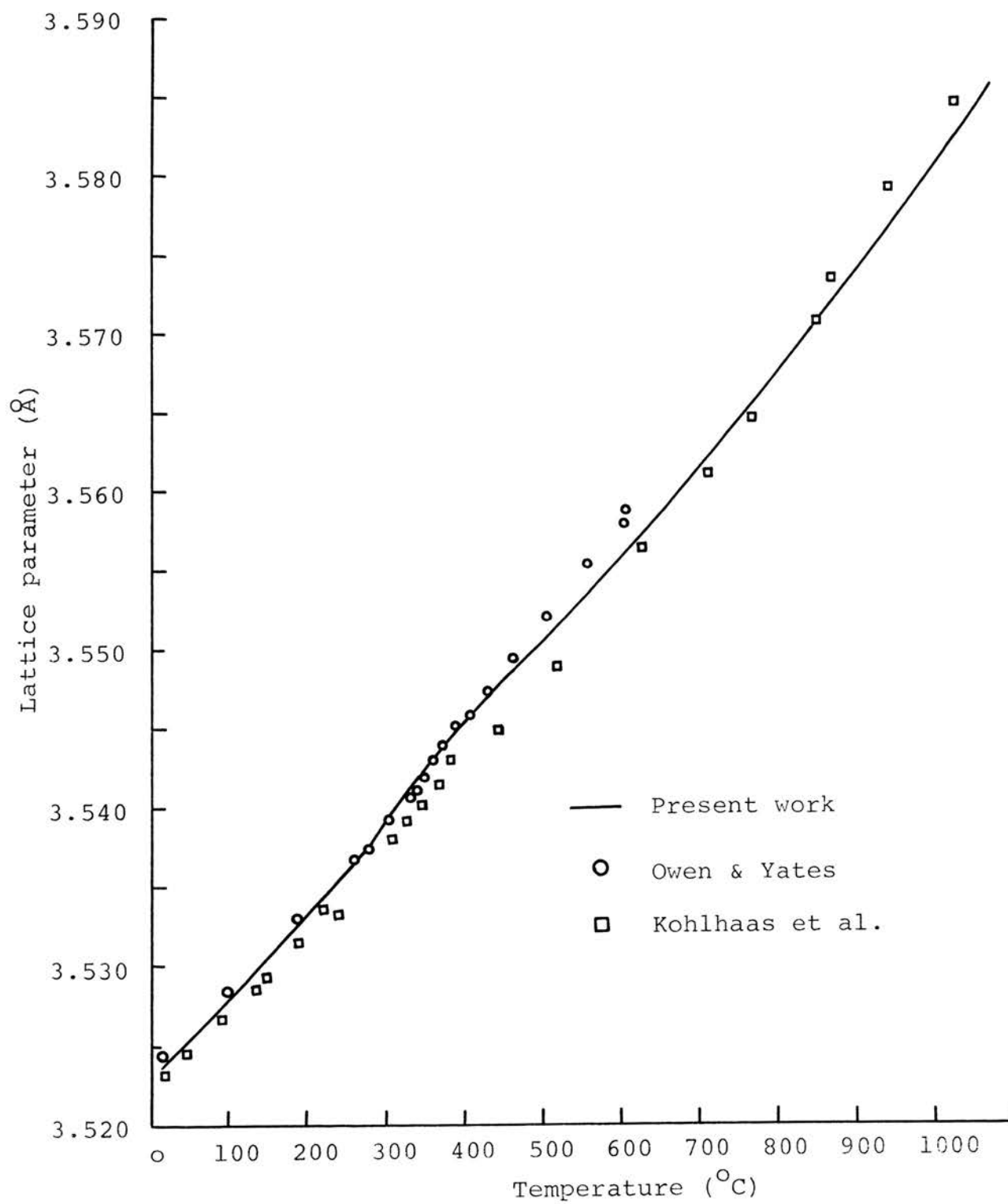


Figure 6 Lattice parameter versus temperature of nickel.

TABLE VI

Thermal expansion coefficients of pure nickel at various temperatures, calculated from Eq. (4), referring to  $a_{25}$ .

Temperature (°C)	Thermal expansion coefficient ( $\times 10^6$ ) °C <sup>-1</sup>
100	15.3
270	17.6
320	21.1
340	20.1
356	18.1
380	13.1
400	12.4
450	14.1
500	15.4
700	16.3
800	16.7
900	19.2
1000	22.1

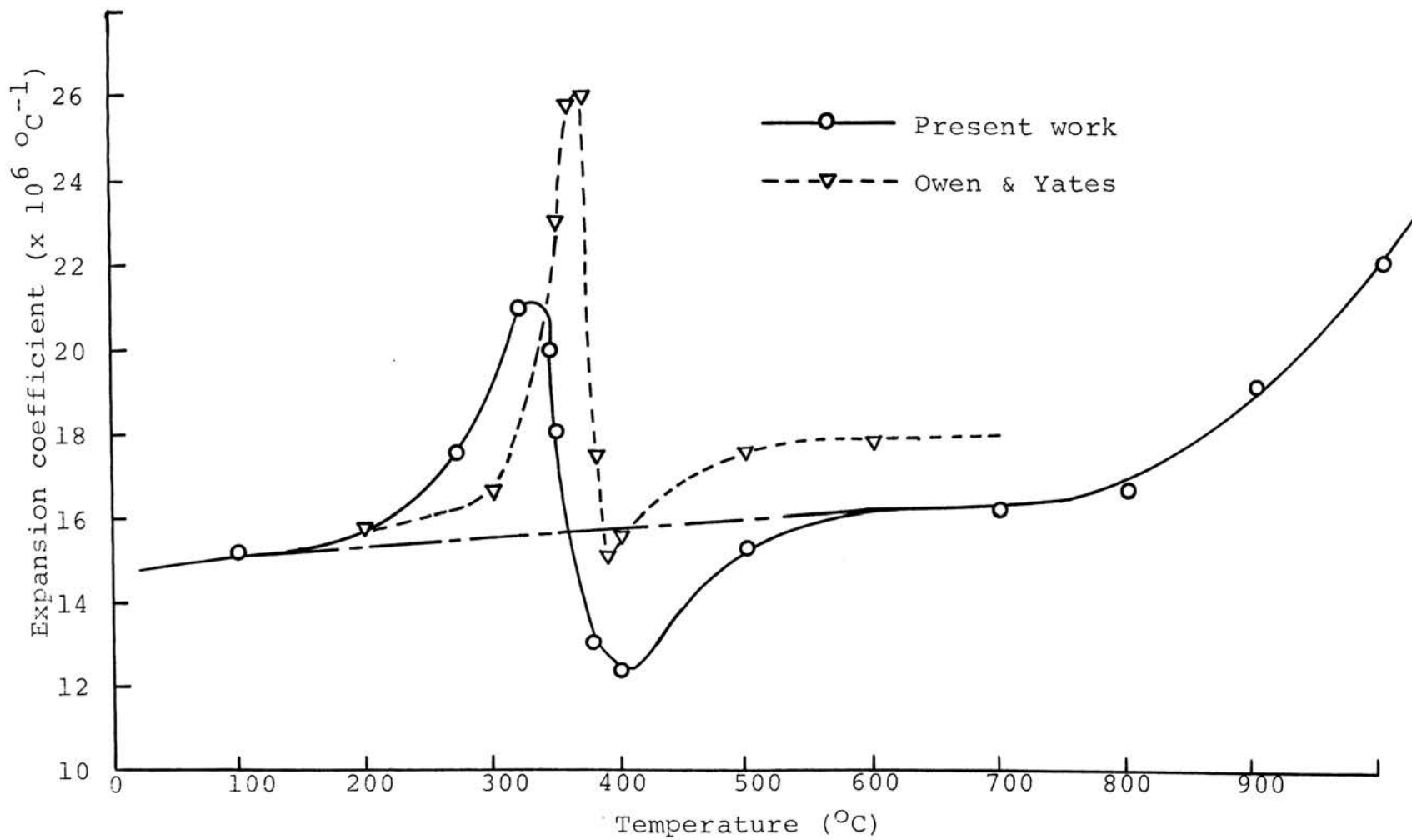


Figure 7 Thermal expansion coefficient versus temperature of nickel.

respectively. The disagreement in the above results can be explained in terms of sample purity. It is a well known fact that impurities strongly affect the magnetic properties of ferromagnetic materials like iron, cobalt and nickel.

As has been shown, the above technique is fairly sensitive and well suited for the investigation of iron: some samples of which display a very distinct Curie point, while others, a very weak Curie point, or none at all.

## PART II

THERMAL EXPANSION OF IRON AND THE INFLUENCE OF NITROGEN  
ON THE LATTICE PARAMETER BETWEEN 25°C AND  
900°C, INCLUDING THE CURIE TEMPERATURE

## CHAPTER IV

## INTRODUCTION AND LITERATURE REVIEW

Comparing the previously reported data regarding the lattice parameter of pure nickel and its expansion coefficients at various temperatures (part I) with those of the literature have shown the reliability of the present experimental technique. Thus a much more difficult problem could be attacked, namely, why some investigators found a change of the expansion coefficient of Fe at the Curie temperature and some did not.

Thermal expansion measurements of iron by the X-ray method have been performed by a good number of investigators. Although the existence of an expansion anomaly of nickel at the Curie point was well established, the position with respect to iron is still in doubt due to the divergent results obtained, as shown by the curves of Fig.8.

The lattice parameter of pure electrolytic and hydrogen reduced  $\text{Fe}_2\text{O}_3$  iron at room temperature was first measured by Hull<sup>(18)</sup>. Then Davey determined the structure of iron in 1924<sup>(19)</sup>. Lattice parameter redeterminations by many investigators followed. On Table VII the results of various authors are collected.

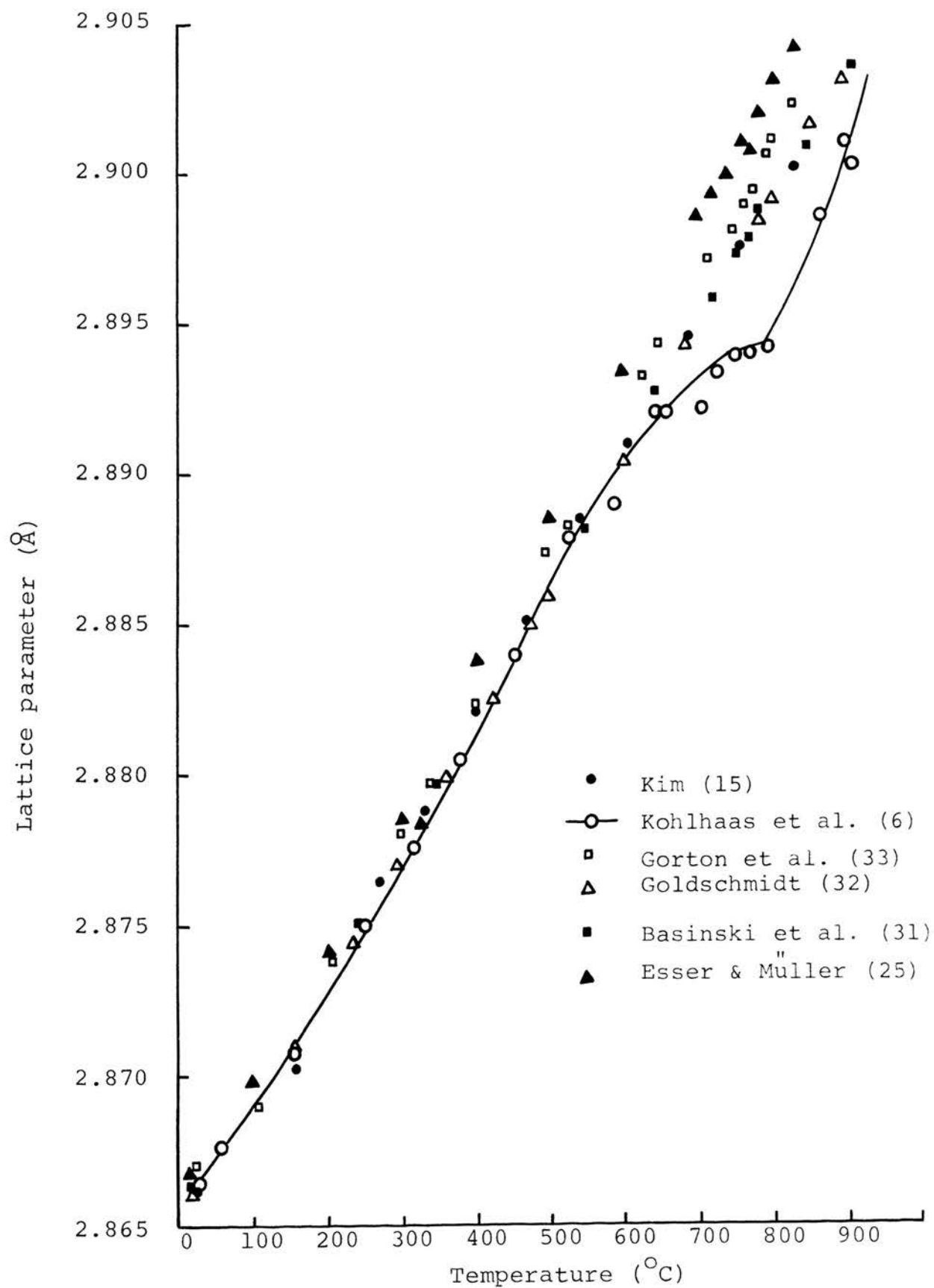


Figure 8 Lattice parameter of pure iron at high temperature (Curie point at 768°C).

TABLE VII

Lattice parameter of alpha iron at room temperature up to the year 1943 (continuation of this table see p52).

Author	Year	a (Å)	Purity
Hull <sup>(18)</sup>	1917	2.86	electrolytic Fe
Davey <sup>(19)</sup>	1924	2.861	chem. pure
Blake <sup>(20)</sup>	1925	2.8661	
Davey <sup>(21)</sup>	1926	2.8661	
Mayer <sup>(22)</sup>	1929	2.865	
Van et al. <sup>(23)</sup>	1931	2.8672	
Bradley & Jay <sup>(24)</sup>	1932	2.8663	
Esser & Müller <sup>(25)</sup>	1933	2.8669	
Owen & Yates <sup>(26)</sup>	1933	2.86675	
Straumanis & Ievins <sup>(27)</sup>	1936	2.8664	
Montoro <sup>(28)</sup>	1937	2.86665	
Hanawalt et al. <sup>(29)</sup>	1938	2.863	
Troiano & McGuire <sup>(30)</sup>	1943	2.8665	

( All lattice parameters are converted from Kx into Å using the conversion factor of 1.00202 )

High temperature measurements were made by Esser and "Müller<sup>(25)</sup>, with three grades of vacuum melted electrolytic iron using cobalt radiation to measure their lattice parameters up to 1100°C. The extrapolation method of Bradley and Jay<sup>(24)</sup> was used to obtain the lattice parameter, extrapolated to 90°. Two of his samples showed lattice parameter anomalies in the Curie temperature region, while with one the anomaly was undetectable. The thermal expansivity was found higher than from preceding dilatometric measurement.

By using a modified Unicam 19-cm-diameter high temperature camera, Basinski et al.<sup>(31)</sup> measured the lattice parameters of 99.969% pure iron between 20 and 1502°C. They concluded that "the forces responsible for ferromagnetism do not affect the interatomic distances by more than 1 part in 10,000."

The measurements in a similar arrangement were repeated by Goldschmidt<sup>(32)</sup> with 99.99% iron powder. His results show an almost perfect linear expansion of iron ( $\alpha = \text{const.}$ ) up to 907°C.

In determining the thermal expansion coefficients of iron and its oxides at elevated temperatures, Gorton et al.<sup>(33)</sup> used a 114.6mm Debye-Scherrer camera arranged for asymmetric

film-loading. The iron sample was electrolytic powder (99.67% iron), hydrogen annealed at 465°C. The data indicated a smooth rise of the lattice parameter of  $\alpha$ -iron with temperature except for the slight dip in the neighbourhood of the Curie transformation (765°C).

Kohlhaas et al.<sup>(7)</sup> made an X-ray investigation of the expansion coefficients of 99.97% polycrystalline iron near the Curie temperature going from room temperature up to the melting point. A distinct anomaly in the expansion at the point of magnetic transformation was observed.

The most successful investigation concerning the lattice parameter and temperature relationship, particularly in the region of Curie temperature, was made by Ridley and Stuart<sup>(34)</sup> with two grades of iron (99.985% and 99.9% pure) having a relatively high oxygen content. A small, but easily detectable lattice parameter anomaly was found at the Curie temperature. The specimens were prepared from filings that passed a 200 mesh B.S. sieve but were retained on a 300 mesh B.S. sieve.

Kim<sup>(15)</sup> used 99.985% iron filings (the same as sample B of this investigation) for his measurement of lattice parameter, but failed to detect the anomalous change of thermal expansion at the Curie point.

In view of the divergent results, the present investigation was undertaken with attention centered around the measurements of the lattice expansion of iron near its Curie temperature.

Austin and Pierce<sup>(35)</sup>, while determining by means of an interferometric method the linear thermal expansion of ten samples of "pure" iron in vacuo from room temperature to 950°C, suggested that at high temperatures the expansion of pure iron is sensitive to impurity traces. Based on this conclusion, the intention of the present work was to study first the influence of pure nitrogen, which occupies almost 80 volume % of the atmosphere. The amount of nitrogen was controlled so that an  $\alpha$ -solid solution could be obtained. Fig. 9 also shows the  $\alpha$ -solid solution region and the Curie temperatures in dependence of the nitrogen concentration.

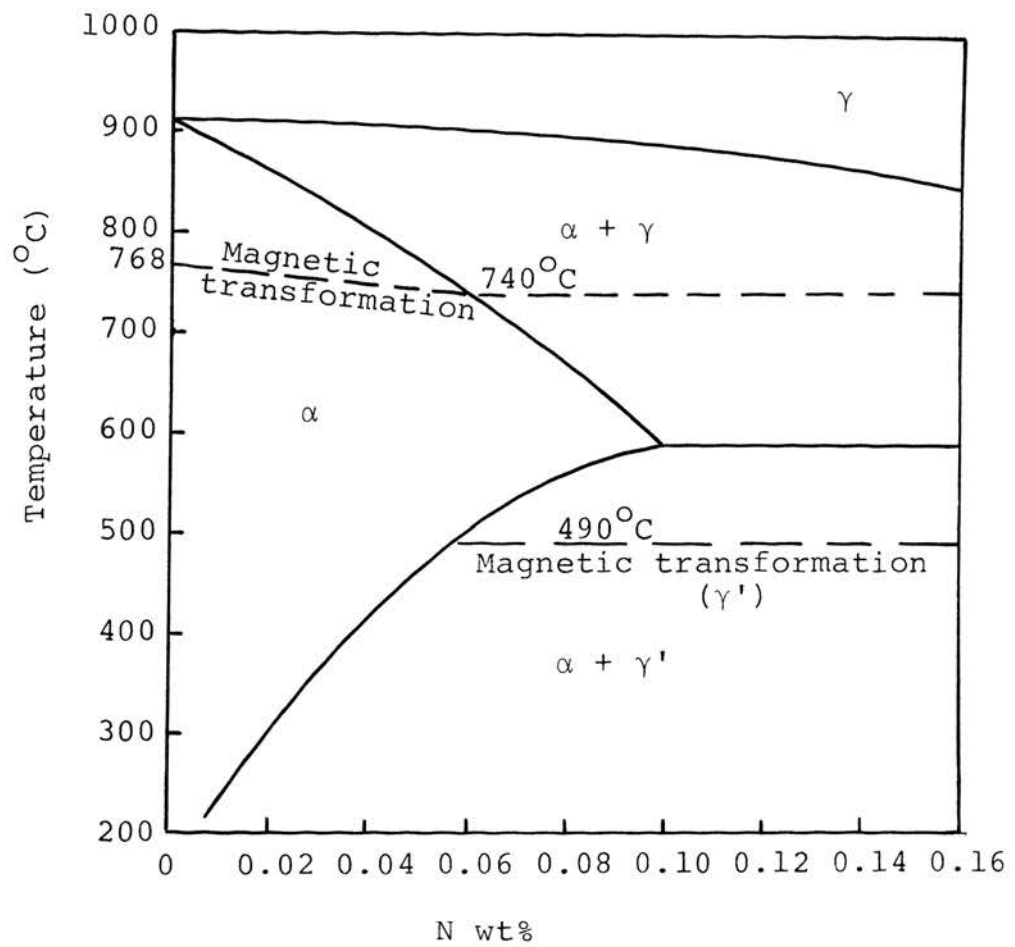


Figure 9 Fe - N phase diagram\*.

\* according to (48) & (49)

## CHAPTER V

## EXPERIMENTAL

## (A) SPECIMEN USED

Three grades of iron were used throughout this part of investigation. Sample A, a very fine powder of 99.999% pure iron, was supplied by the Leico Industries, Inc. A typical analysis on metallic basis is as follows:

		<u>p.p.m.</u>
Manganese		3
Silicon		3
Magnesium		2
Copper	<	1
Silver	<	1

Sample B is a high purity zone-refined iron (99.985%) which was used previously by Kim<sup>(15)</sup> for his X-ray work. In Table VIII a typical analysis of this sample is given. Details are in Kim's thesis<sup>(15)</sup>.

Sample C, 99.9% pure iron, was received from Koch-Light Lab., LTD, England (Batch No. 38536). It contains small amounts of nickel and traces of carbon, nitrogen and oxygen. When these elements are removed (by heating the sample under vacuum or in a hydrogen atmosphere), iron in a very pure form

TABLE VIII

Analysis of high purity zone-refined iron.  
(Sample B)

Impurity	im p.p.m.	Impurity	in p.p.m.
Al	15	Ni	20
Sb	5	p	9
As	5	Si	10
Bi	0.2	Sn	5
B	5	Ti	1
Cd	5	W	5
Ca	10	V	10
Cr	5	Zn	1
Co	5	Zr	1
Cu	7	H <sub>2</sub>	0.2
Pb	1	S	5±3
Mg	5	O <sub>2</sub>	1.7
Mn	0.5	C	9±4
Mo	5	N <sub>2</sub>	0.2

Total impurity content was : 152 p.p.m. (99.985% Fe)

remains. The average particle size of the powder was  $7\mu$ .

#### (B) SAMPLE PREPARATION

Although thermal charging of iron by nitrogen is slow due to the formation of a nitride layer on the surface of the Fe grains, nevertheless, it was expected that by employing a very fine iron powder it will still "absorb" nitrogen to some extent.

(a) Nitrogen charging The high purity sample A was assumed to be free of any gas and was used to prepare the sample in the  $\alpha$ -solid solution region (Fig. 9). 0.4g of the iron powder were placed in a pyrex tube (about 15cm long and 0.8mm of i.d.) with one end sealed. A neck was made somewhere about 5 cm from the closed end of the tube. Then the tube was connected to a mechanical pump, evacuated and a known amount of pure nitrogen, as read from a monometer was introduced into the tube. Fig. 10 shows the arrangement for filling the tube with nitrogen. Finally, the tube was sealed at the neck, its volume estimated, heated in an electric furnace at about  $600^{\circ}\text{C}$  for a predetermined time, and then air-cooled. Three samples with different amounts of nitrogen heated for various periods were prepared. (see Table X, p. 50)

- A - monometer  
B - Sample in the pyrex tube  
C - nitrogen tank  
D - mechanical pump
- \* All connections are made by plastic tubing.

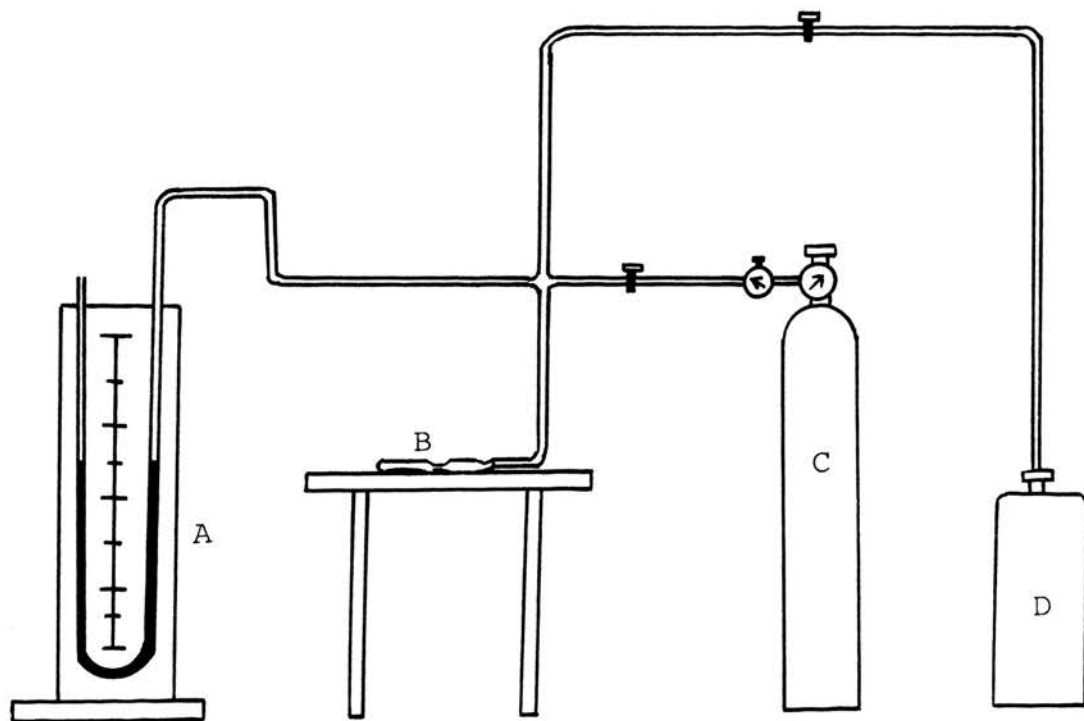


Figure 10 Schematic diagram of filling the tube containing of Fe with nitrogen.

(b) Analysis of nitrogen in iron It is clear that the iron samples contained both the "absorbed" or dissolved nitrogen and the nitride on the surface of the fine iron granules. Since, sharp X-ray diffraction lines were obtained of samples placed in fine capillaries, it is believed that the concentration of N leveled out throughout the sample (by diffusion) when it was exposed to high temperatures inside the X-ray camera. Due to the probability that not all the  $N_2$  present in the "nitrogen charging" tubes reacted with Fe, it became necessary to analyse the sample for their total N content.

For the determination of gases in metals, there are usually two distinct operations: the extraction of the gas from the metal and the determination of the volume of the extracted gas. The hot vacuum extraction technique was employed in the present study since it is better than any other for the determination of N or H in steels<sup>(15)</sup>.

(1) Gas analyzer: A Leco Hydrogen Analyzer (No. 534-600) which works on the principle of hot vacuum extraction was modified for nitrogen analysis by removing the catalyst (hot copper oxide) and the anhydron. A schematic of the analyzer is shown in Fig. 11. The gas extracting and measuring parts are shown to the left and the right side, respectively, of the diagram. Before dropping the preweighed sample in its stainless steel

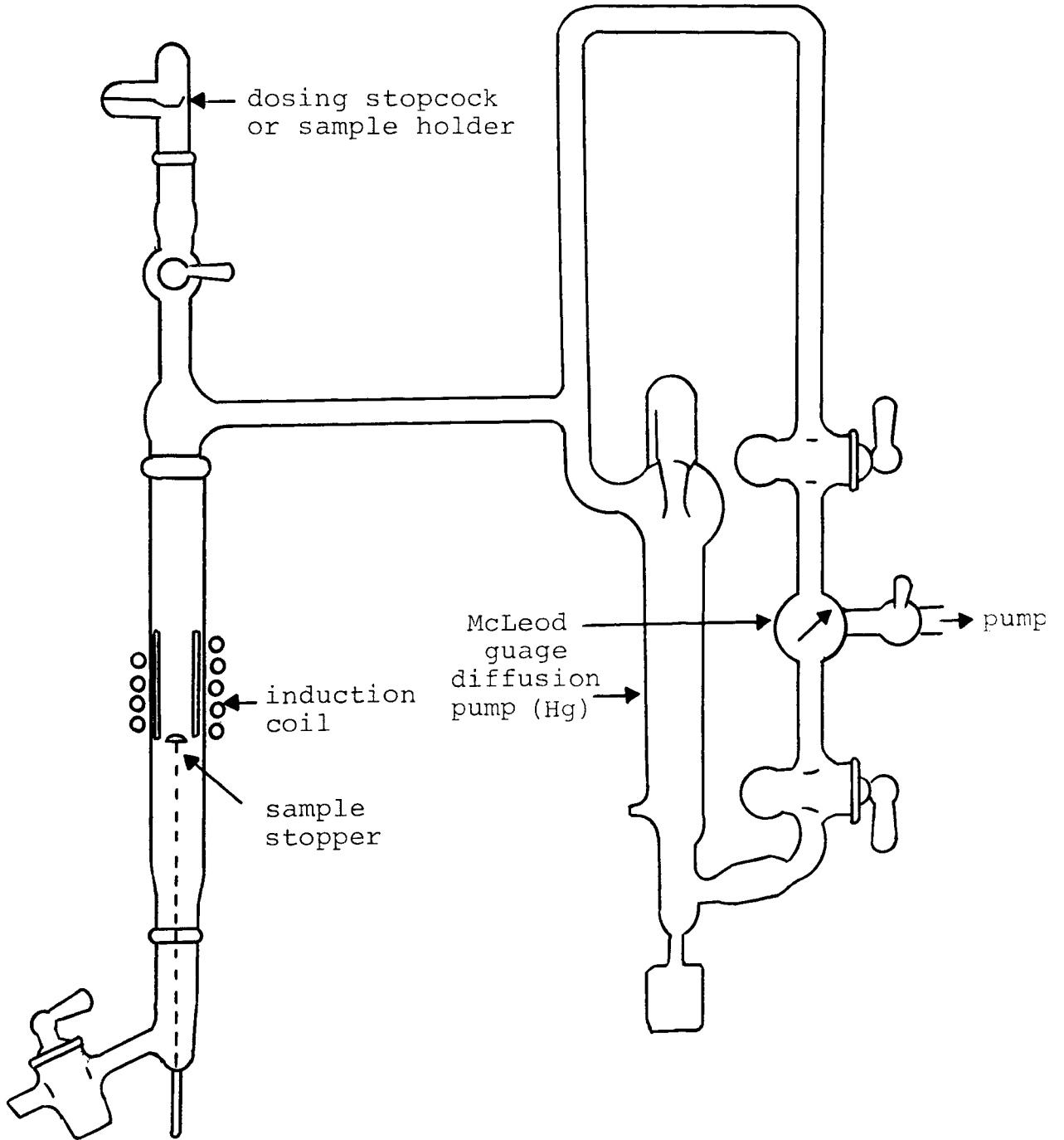


Figure 11 Schematic diagram of the Leco gas analyzer.

crucible from the sample holder (in vacuum) into the furnace, it was necessary to turn the induction furnace on for several hours at 900°C to get rid of the absorbed gases on the walls of the glassware of the instrument. By a mercury diffusion pump, the gas liberated by the sample is forced into the analyzing part and the pressure measured by a McLeod gauge.

(2) Calibration of the furnace temperature and check of the volume of the system: By introducing a known amount of dry air of atmospheric pressure into the system and by measuring the new resulting pressure, the volume of the system can be found from the following equation:

$$V = P_1 V_1 / P \quad (\text{at a constant } T) \quad (6)$$

where  $V$  is the volume of the system,  $P$  - the pressure measured,  $P_1$  - the atmospheric pressure read from barometer and  $V_1$  - the known amount of the admitted dry air. At operation conditions, it was found that the system has a volume of  $338 \pm 7 \text{ cm}^3$ . (see Table IX)

Temperature measurement of the sample was achieved with an optical pyrometer directed to the crucible within the induction coil. The furnace temperature was adjusted by a variable transformer. The relationship between the temperature of the crucible and the dial reading of the voltage delivered by the variable transformer was established, assuming that temperature equilibrium has

TABLE IX

Determination of the volume of the system(gas analyzer).

Known amount of air ( $V_1$ cm <sup>3</sup> )	Atmospheric Press. ( $P_1$ mm)	Measured P (mm)	System vol. V (cm <sup>3</sup> )
0.05560 x 4	732.8	0.500	326
0.05560 x 5	732.8	0.600	340
0.05560 x 6	732.8	0.720	340
0.05560 x 4	732.4	0.520	313
0.05560 x 5	732.4	0.610	334
0.05560 x 6	732.4	0.728	336
Average:			331 ± 7* (cm <sup>3</sup> )
Calibration**:			7
			338 ± 7 (cm <sup>3</sup> )

\* Using equation (6), page 21.

\*\* The volume of the dosing stopcock is smaller than that of the sample holder by 7 cm<sup>3</sup> (Fig.11). In operation, the volume of the system was increased by 7 cm<sup>3</sup>.

been reached. The temperature of the crucible was kept at about 930°C. Fifteen minutes extraction at this temperature was sufficient, as there were no further pressure increases in the analyzing part (Fig. 11) beyond this period of time.

(3) Sample analysis and calculation: As the weighed sample was in powder form, its analysis was achieved by filling it into a stainless crucible (6mm in diameter and 20mm in height) which was degassed before each run. The amount of nitrogen in the Fe was calculated from the following equation:

$$\text{Nitrogen in p.p.m.} = (PVM \times 1000) / RTW \times 760 \quad (7)$$

where P is the pressure read from the McLeod gauge in microns, V the precalibrated volume of the system (338cm<sup>3</sup>), M the molecule weight of nitrogen (28.8), R the gas constant (0.08204 l-atm/deg. mole = 82.05 cm<sup>3</sup>-atm/deg. mole), T the absolute temperature in degree Kelvin, and W the weight of the sample (0.400g). The results are summarized in Table X (calculations are made in the Appendix, p. 84-86).

As can be seen from the Table X, the measured value of N in Fe is comparable with the calculated (maximum) value. The slightly higher measured value of sample D may be due to contamination by gases, such as hydrogen, in the high purity iron powder. In each case, the values are within the limit of experimental error.

TABLE X

Sample D, E and F, prepared from 0.4 g of sample (A)  
 (99.999% Fe) charging it with various amounts  
 of N<sub>2</sub> at 630°C for various time periods.

Sam- ple	N <sub>2</sub> vol. cm <sup>3</sup>	N <sub>2</sub> cm Hg	Heat. time hr.	N <sub>2</sub> cal. in %	N <sub>2</sub> found* in % or in p.p.m.
D	2.76	2	36	0.021	0.022 or 220
E	2.51	3	12	0.029	0.017 or 170
F	2.66	3	6	0.029	0.011 or 110

\* See Appendix, p.84 - p.86

## (C) EXPERIMENTAL RESULTS

By using cobalt radiation (wavelength  $K\alpha_1 = 1.78892 \text{ \AA}$ ) and the (310) X-ray diffraction line, the precise lattice parameters of the three iron samples were determined as well as of those charged with N. The choice of the radiation, the indexing of the X-ray pattern<sup>(15)</sup>, the preparation of the sample for X-ray work and the measurement of the film etc. are described in the preceding part. The  $K\alpha_2$  line of (310) was disregarded due to lower intensity.

(a) Lattice parameter at room temperature Precise lattice parameters of pure iron at room temperature were determined using the asymmetric film loading method. The results are collected in Table XI, together with previously published data, where the purity of Fe was mentioned. The lattice parameter of the three grades of iron determined in this investigation are generally close to that of pure iron determined by previous workers. The slight difference between present values and previous ones may be within the limit of experimental errors.

The lattice parameter of sample B ( $a_{25} = 2.86624 \text{ \AA}$ ), 99.985% pure iron, is in excellent agreement with that determined by Kim<sup>(15)</sup>, who used the same sample and technique and reported a value  $2.86623 \text{ \AA}$  at the same temperature.

TABLE XI

Lattice parameter of pure iron determined between 1935-71.

Author	$t^{\circ}\text{C}$	$a_t$ (Å)	$a_{25}^*$ (Å)	Remark (Fe%)
Jette & Foote <sup>(36)</sup>	25	2.86624	2.86624	0.007% C & 0.004% each of Si, S & O
Van Bergen <sup>(37)</sup>	20	2.86651	2.86668	99.96
Lu & Chang <sup>(38)</sup>	20	2.8663	2.8664 <sub>7</sub>	99.96
Thomas <sup>(39)</sup>	20	2.8664 <sub>5</sub>	2.8666 <sub>2</sub>	
Kochanovska <sup>(40)</sup>	25	2.8667	2.8667	
Swanson et al. <sup>(41)</sup>	25	2.8664	2.8664	99.9974
Grønvold et al. <sup>(42)</sup>	20	2.8663	2.8664 <sub>7</sub>	
Owen & Williams <sup>(43)</sup>	18	2.8662	2.8664	99.98
Sutton & Hume- Rothery <sup>(44)</sup>	20	2.86621	2.8664	99.969
Basinski et al. <sup>(31)</sup>	20	2.86628	2.8664	99.969
Goldschmidt <sup>(32)</sup>	20	2.8662	2.8663 <sub>7</sub>	99.99
Gorton et al. <sup>(33)</sup>	22	2.8663	2.8664	99.67
Kohlhaas et al. <sup>(6)</sup>	20	2.8665	2.8666 <sub>7</sub>	99.97
Ridley & Stuart <sup>(34)</sup>	20	2.8662	2.8663 <sub>7</sub>	99.999
Straumanis & Kim <sup>(45)</sup>	25	2.86623	2.86623	99.985
Present work	25	2.86621	2.86621	99.999
Present work	25	2.8663	2.8663**	99.999
Present work	25	2.86624	2.86624	99.985
Present work	25	2.8663	2.8663**	99.985
Present work	25	2.86614	2.86614	99.9
Present work	25	2.8663	2.8663**	99.9

\* Reduced by use of the expansivity of  $3.46 \times 10^{-5} \text{ Å}/^{\circ}\text{C}$ \*\* Determined in the high temp. camera, error  $\pm 0.0002 \text{ Å}$

(b) Lattice parameters and expansion coefficients at elevated temperatures The thermal expansion coefficients of the samples were determined from the plot of lattice parameter versus temperature, using equations (4) & (5), by finding the slope of the curve at  $t^{\circ}\text{C}$  and dividing them by the respective lattice parameters (in present case,  $a_{25}$  was used as reference).

The thermal expansion of pure iron from room up to  $A_3$  point temperature were determined. The results are collected in Table XV, Table XVI and Table XVII, p75-p79, and plotted respectively in Fig. 12 through Fig. 17, which clearly show the definite influence of magnetostrictive part on the thermal expansion of pure iron. It can be seen that a small, but detectable expansion anomaly exists in all three cases over a temperature range of about  $30^{\circ}\text{C}$  at Curie point region ( $770^{\circ}\text{C}$ ). In Fig. 13, 15 and 17 the region around the Curie point is drawn in an enlarged scale. The thermal expansion coefficients versus temperature are also plotted on these three figures.

In Table XII, the experimental results of the thermal expansion coefficients of pure iron are summarized and compared with previous ones. As shown in Fig. 18, the expansivity of pure iron increase from room temperature, reaches a maximum at about  $500^{\circ}\text{C}$  and then becomes constant before abruptly falling to a minimum at about  $770^{\circ}\text{C}$  (the Curie point).

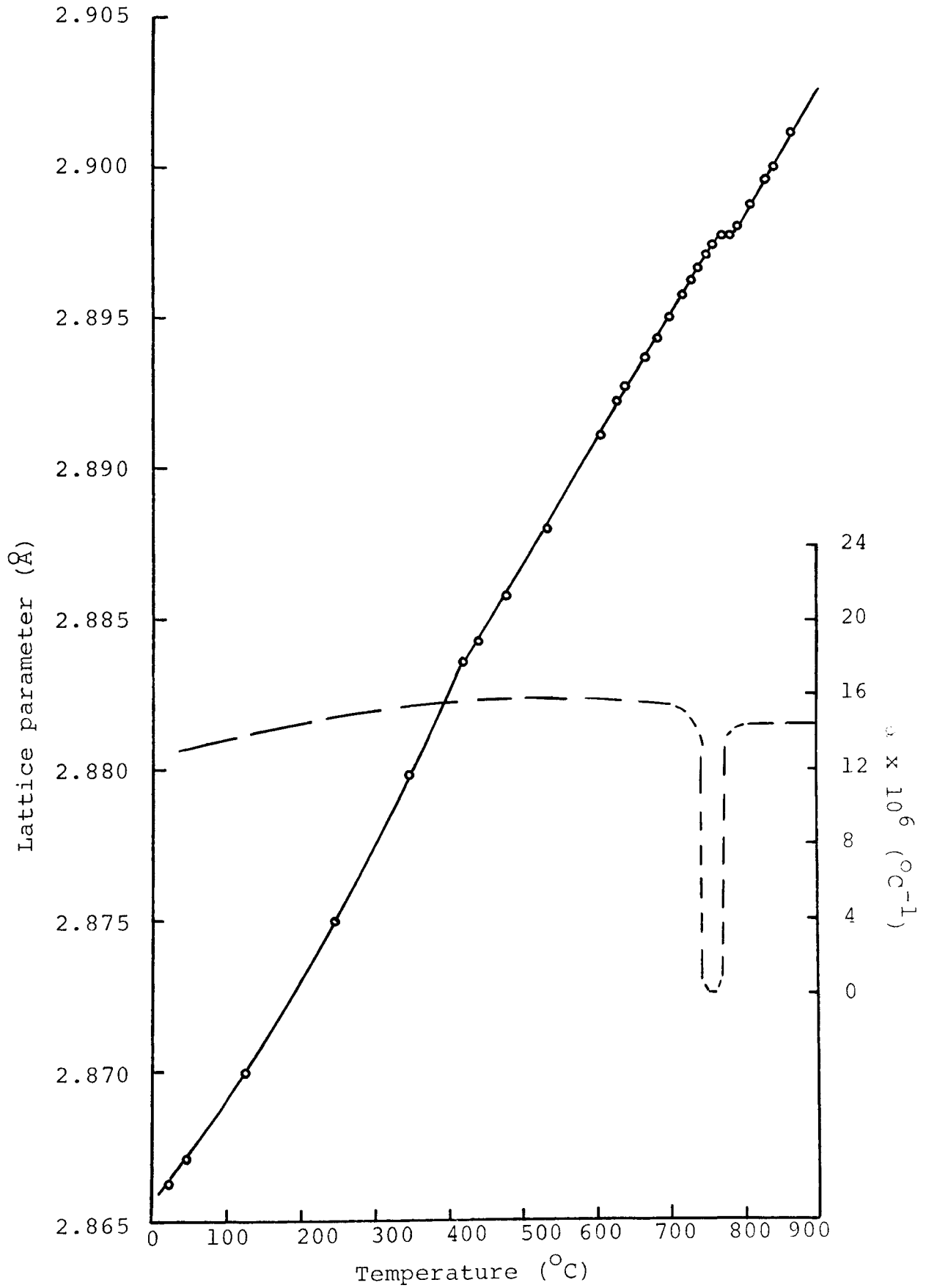


Figure 12 Lattice parameter and  $\alpha$  of Sample A, 99.999% Fe at various temperatures.

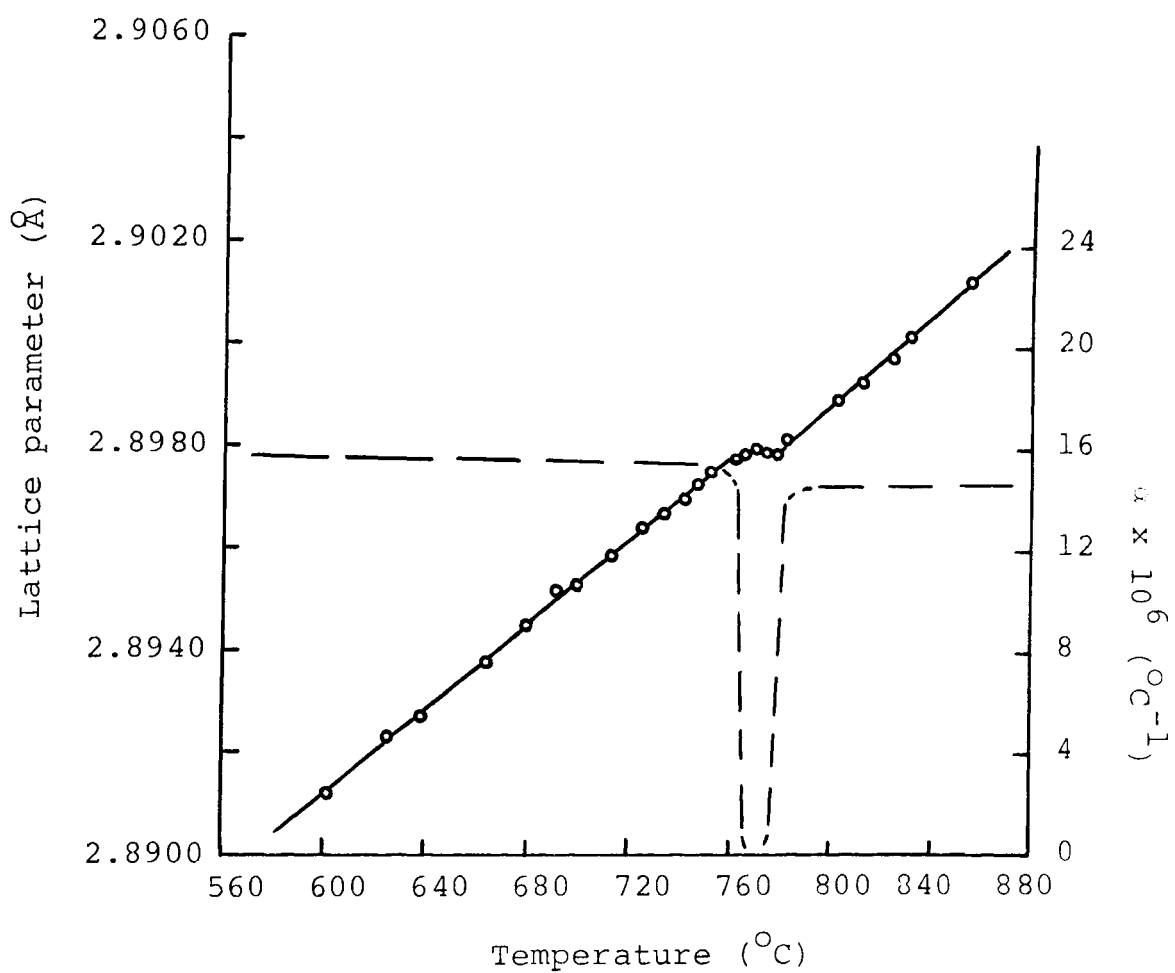


Figure 13 Lattice parameter and  $\alpha$  of Sample A, 99.999% Fe at the Curie temperature. Expansion coefficient  $\alpha$ -to the right.

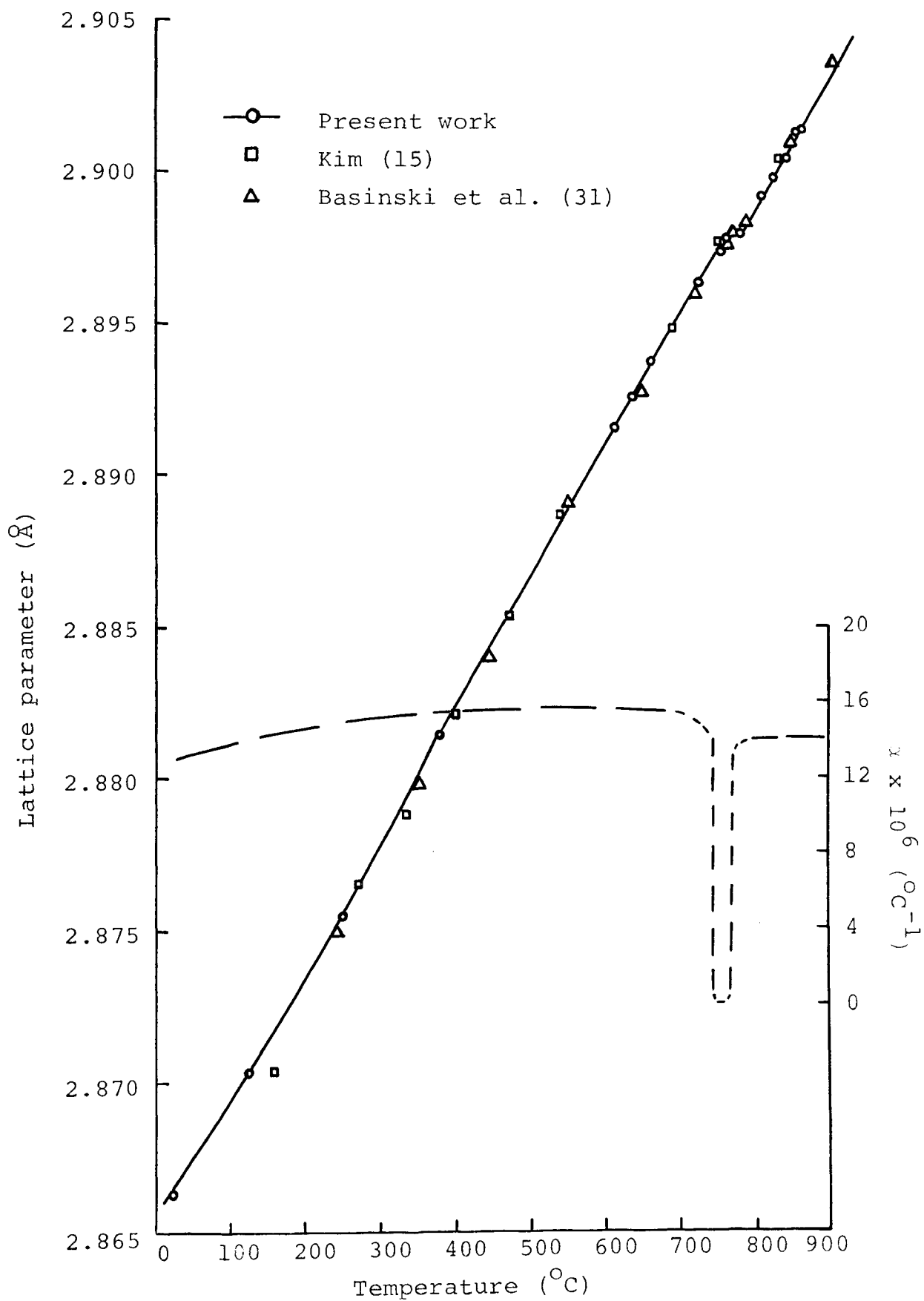


Figure 14 Lattice parameter and  $\alpha$  of Sample B, 99.985% Fe at various temperatures.

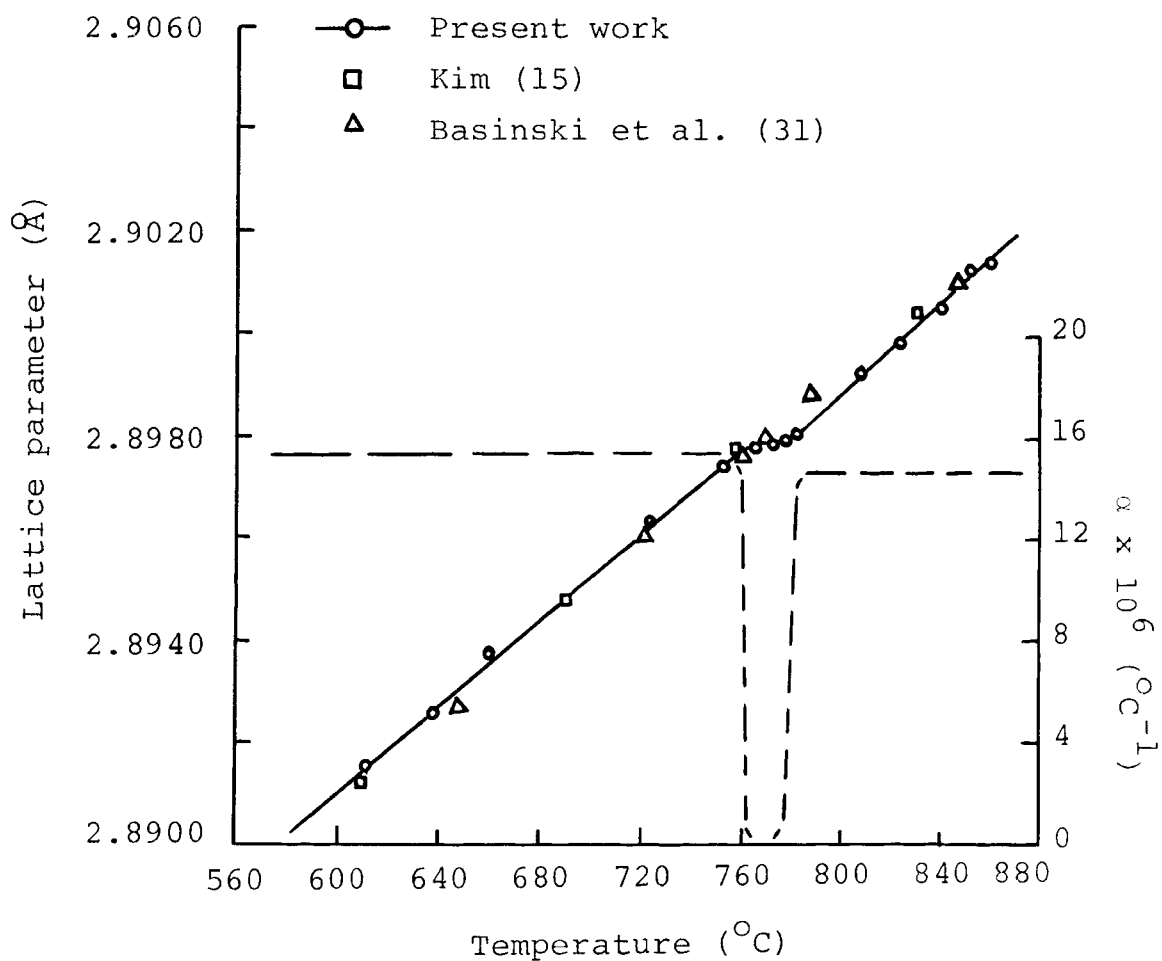


Figure 15 Lattice parameter and  $\alpha$  of Sample B, 99.985% Fe at the Curie temperature. Expansion coefficient  $\alpha$  - to the right.

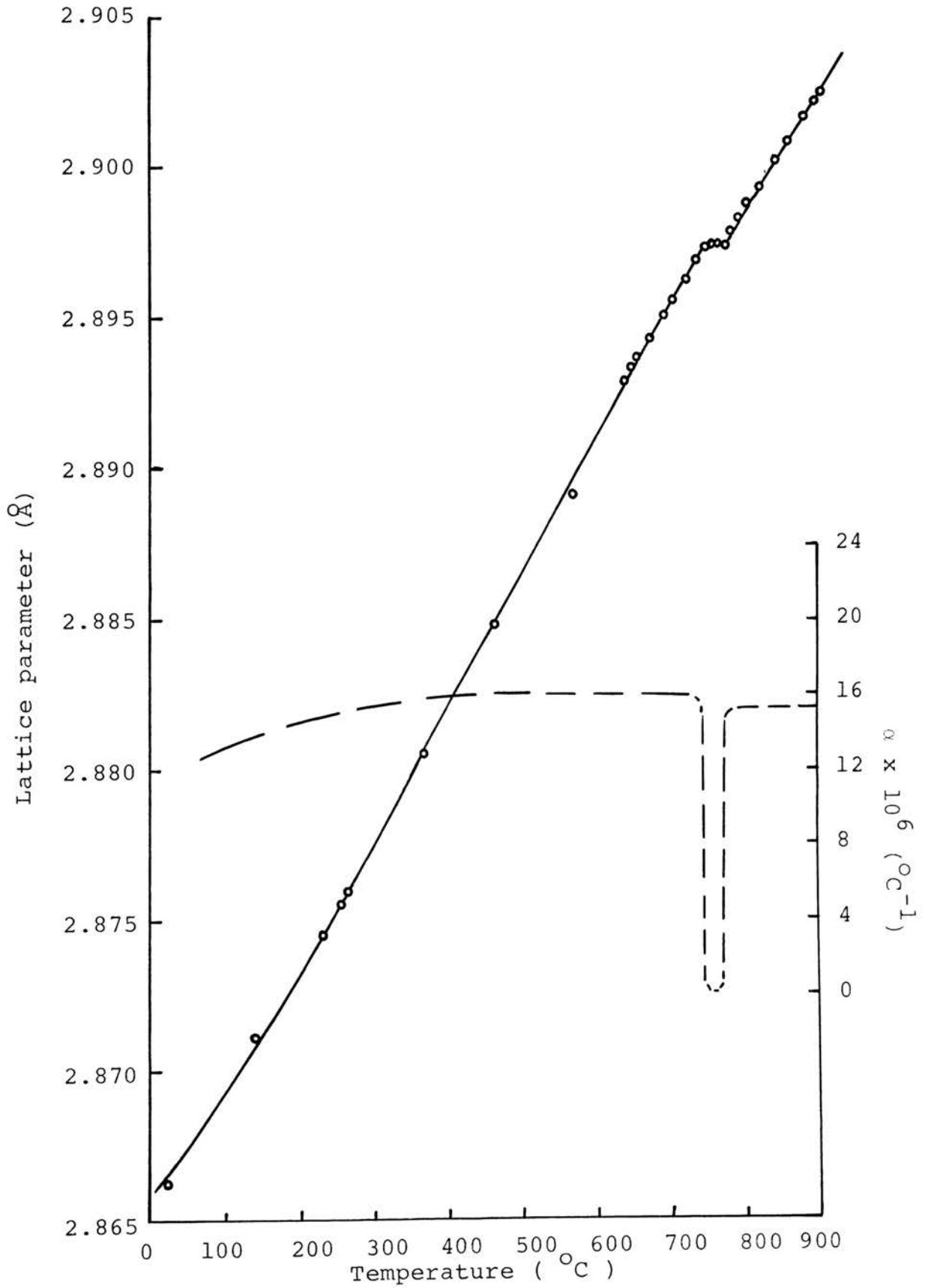


Figure 16 Lattice parameter and  $\alpha$  of sample C, 99.9% Fe at various temperatures.

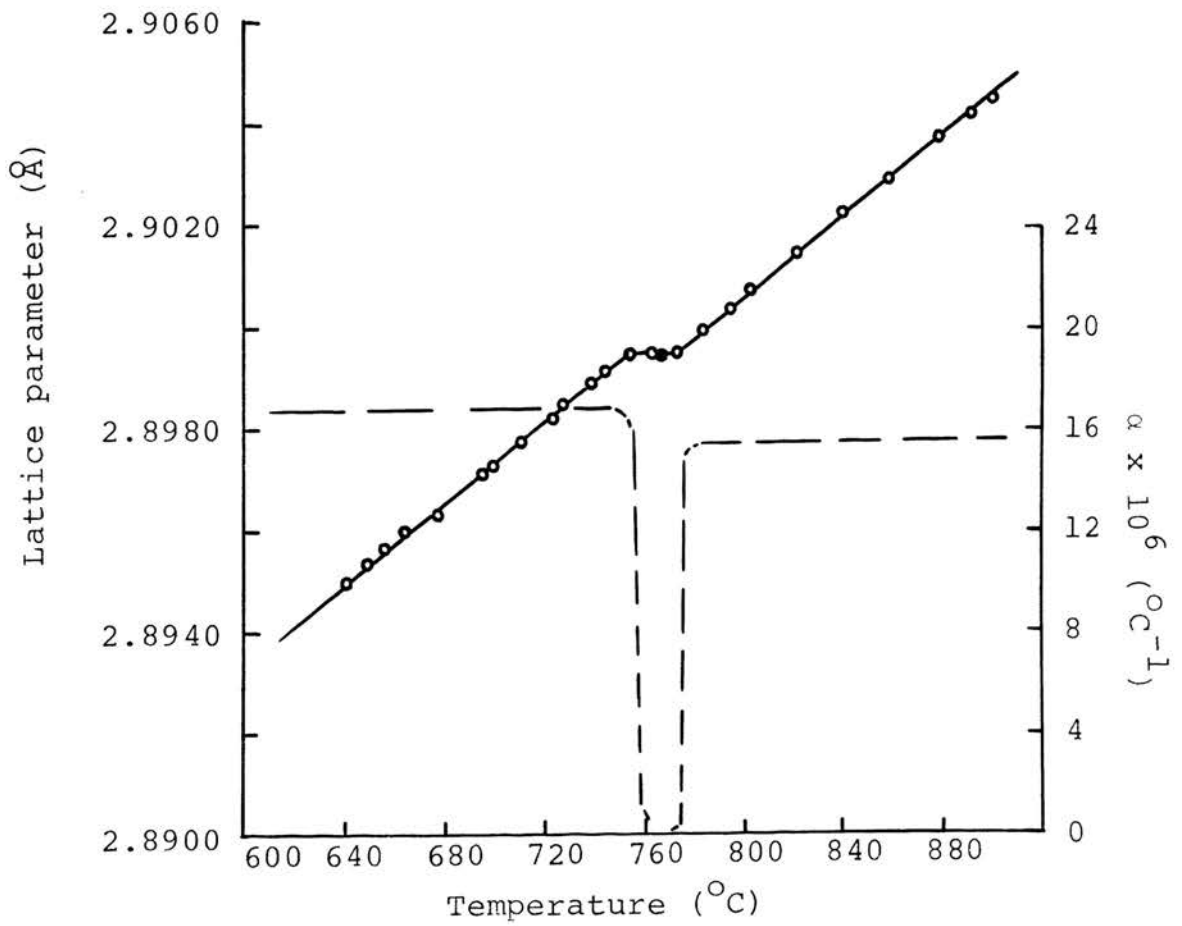


Figure 17 Lattice parameter and  $\alpha$  of sample C, 99.9% Fe at the Curie temperature

TABLE XII

Coefficient of linear thermal expansion of  
pure iron  $\alpha \times 10^6$  (millionths per  $^{\circ}\text{C}$ ).

Temp. ( $^{\circ}\text{C}$ )	(A & B)*	(C)*	(G)	(H)
100	13.8	12.2	13.3	12.5
200	14.3	15.5	14.5	14.0
300	15.0	16.6	15.5	15.3
400	15.7	16.8	16.2	16.1
500	15.9	16.8	16.2	16.5
600	15.5	16.8	15.8	16.4
700	15.5	16.8	15.8	15.8
Curie pt. 768 $^{\circ}\text{C}$	0	0	-	-
800	14.5	15.5	15.4	15.7

\* Coefficients go to zero between 760 - 770 $^{\circ}\text{C}$ .

(A & B) Present work, sample A & B

(C) Present work, sample C

(G) Hidnert<sup>(45)</sup>

(H) Lehr<sup>(46)</sup>

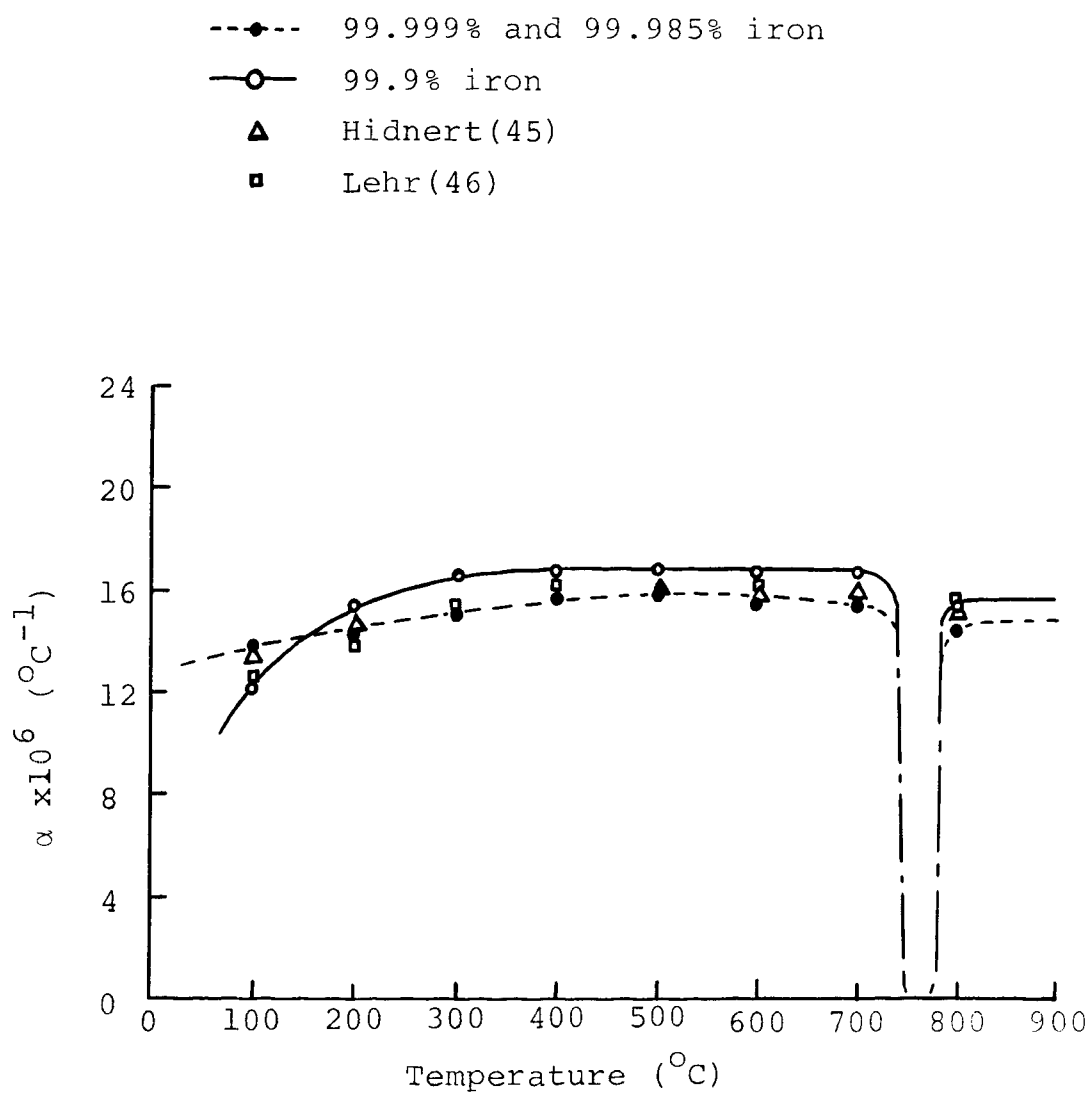


Figure 18 Variation of thermal expansion coefficient with temperature for pure iron.

The sudden decrease of thermal expansion coefficient corresponds to the anomalous change of lattice parameters of that temperature range.

The results of the thermal expansion measurements of the three Fe samples containing different amounts of nitrogen are collected in Table XVIII, Table XIX and Table XX , p80-p83, and plotted in Fig. 19 and Fig. 20. The results revealed two facts: (1) that contrary to the supposed small solubility of nitrogen in  $\alpha$ -iron, the very fine and pure Fe powder absorbs detectable amounts of nitrogen even under low pressure (2-3cm Hg) and (2) that these small amounts of nitrogen decrease considerably the  $a$ -parameter particularly at the Curie point and that this influence increases with the amount of N in the iron.

By using the high-temperature camera, at room temperature nitrogen was found to have no effect (within the limits of error) on the lattice parameter of iron.

The thermal expansion coefficients of the three nitrogen-containing Fe samples were also determined by the mentioned Eq. (4) & Eq. (5). The data are summarized in Table XIII, which are plotted in Fig. 19 and Fig. 20 respectively. It is apparent that nitrogen has a definite influence on the expansion coefficient of iron at elevated temperatures.

TABLE XIII

Thermal expansion coefficient of Samples D,  
E and F above 600°C.

Temperature (°C)	$\alpha \times 10^6$ (°C <sup>-1</sup> )		
	(D)	(E)	(F)
600-700	14.4	14.4	13.8
745	0	2.4	13.8
750	2.4	5.0	13.8
765	10.9	12.2	9.6
770	39.0	29.9	14.0
780-900	14.0	14.0	14.0

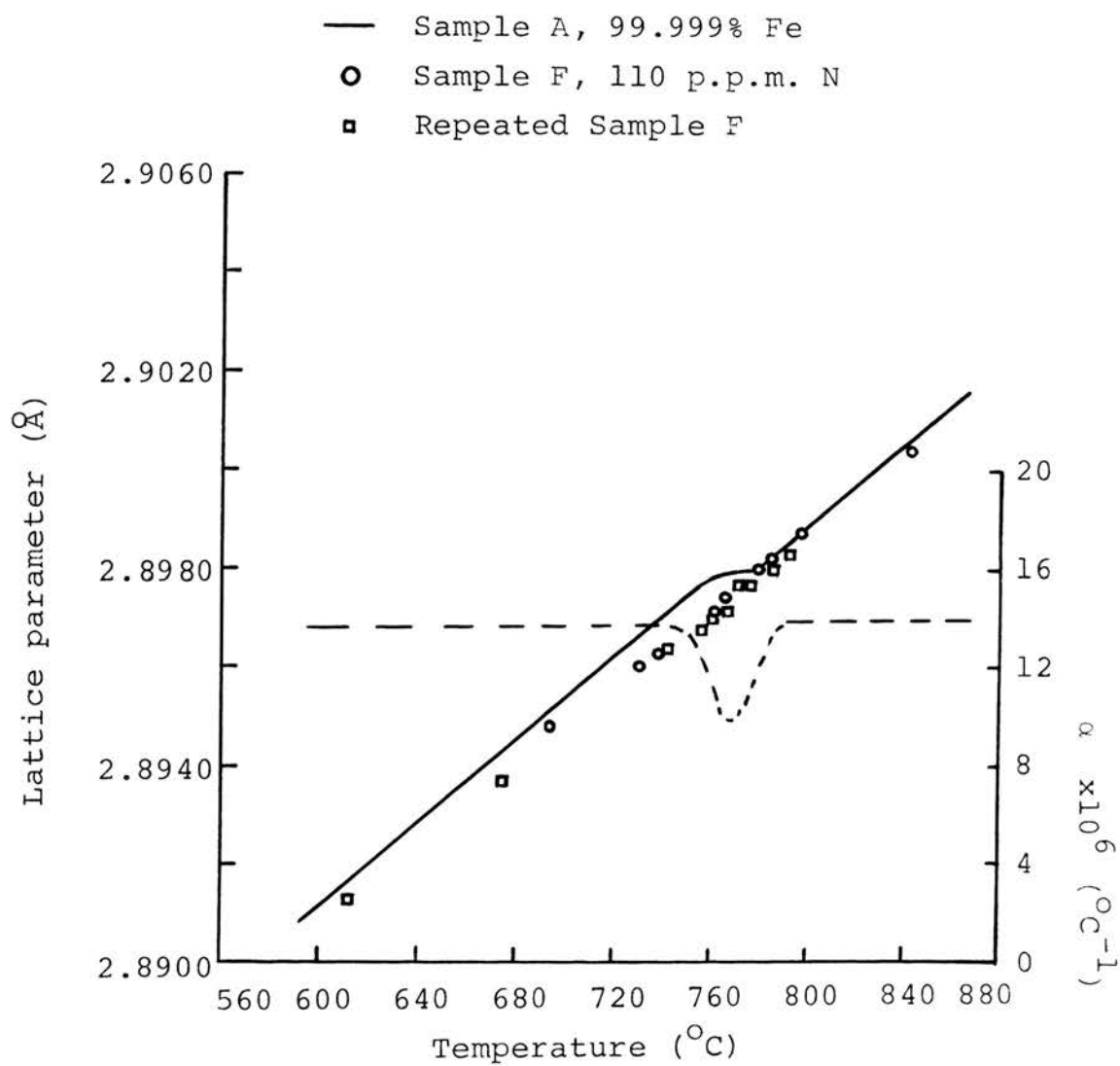


Figure 19 Effect of 110 p.p.m. nitrogen on the lattice parameter of pure Fe. (The slight change of  $\alpha$  within 760-780°C might be within the limits of error.)

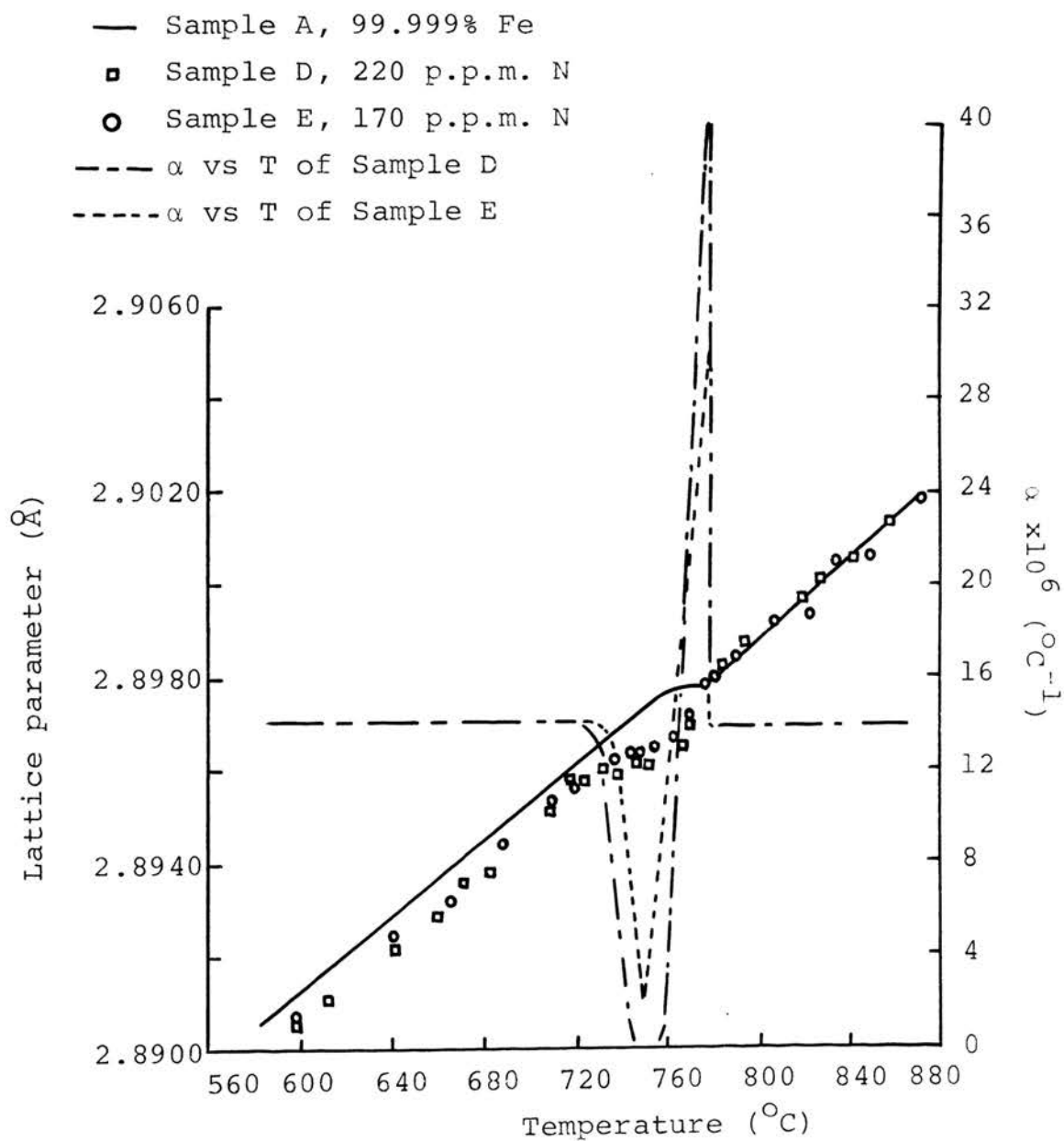


Figure 20 Effect of nitrogen on the lattice parameter of pure Fe.  
 The thermal expansion coefficient  $\alpha$  (right side) of samples D and E.

## CHAPTER VI

## DISCUSSION

The present measurements on sample A and sample B at elevated temperature seem in very good agreement with the results of Ridley and Stuart<sup>(34)</sup>, who paid particular attention to the trend of lattice parameters around the Curie temperature and determined the anomaly in thermal expansion. The failure of Kim<sup>(15)</sup> and Basinski et al.<sup>(31)</sup> to observe the anomalous expansion of iron is maybe due to lack of sufficient density of lattice parameter measurements in the region of the Curie point. This can be clearly seen from Fig.14 (also Fig.15) : there is a good agreement between the present measurements and those of Kim and Basinski et al., except one experimental point, which eliminates the horizontal part of the curve at the Curie point. It may also be that the Fe used by Kim had a slightly different composition than the present sample, although prepared from the same piece of the zone refined iron. As can be followed from the Fe containing some N, the a-parameter at the Curie point is very sensitive to certain impurities.

Fig.19 and Fig.20 show the thermal lattice expansion of nitrogen-charged iron and of pure iron (sample A) in the region of Curie temperature. The curves indicate that nitrogen has a definite influence on the lattice parameter

of pure iron, decreasing it at elevated temperatures. However, this gas has no effect at room temperature (see Table XVIII and Table XIX).

The thermal expansion coefficient of the iron-N solid solutions is lower at elevated temperature (up to Curie point) and the extent of this lowering increased with the concentration of nitrogen in  $\alpha$ -iron (Fig.20). The Curie temperatures were also slightly lowered with the increase of N content: 760, 755 and 750°C respectively. This is in accord with Fig.9 which shows that increasing amounts of N in Fe lower the Curie temperature. Estimations from Fig.9 are that the Curie points of sample D, E and F are 763, 760 and 758 respectively. This behavior also confirms that the N-containing Fe samples are  $\alpha$ -solid solutions. No strange lines (of a second phase) could be observed on the X-ray patterns of the three N-containing samples.

Referring to fact (1), page 62, the another source of nitrogen in  $\alpha$ -iron might be from the decomposition of nitride during the high-temperature (above 600°C) X-ray experiment, since iron nitride is unstable and tends to decompose at elevated temperature.

Above 780°C all the lattice parameters of the N-containing Fe coincide with those of pure iron (See table XIV).

TABLE XIV

Lattice parameters of pure Fe (samples A, B & C)  
and of N-containing Fe (samples D, E & F), a in  
Å of samples above 780°C.

T(°C)	(A)	(B)	(C)	(D)	(E)	(F)
780- 783	2.8982	2.8981	2.8980	2.8981	2.8980	2.8980
784- 785	2.8983			2.8983	2.8980	2.8980
793	2.8989					2.8983
794- 795			2.8984	2.8988		
801	2.8990		2.8987			
812	2.8993					
820- 821			2.8995	2.8997		
824- 825	2.8998	2.8999			2.8994	
831	2.9002					
835					2.9003	
840- 843		2.9006	2.9003	2.9006	2.9006	2.9004
852		2.9014				
856- 859	2.9013		2.9010	2.9014	2.9013	
875						2,9020
877					2.9019	
879				2.9018		
890				2.9023		
$\alpha \times 10^6$	14.0	15.4	14.3	14.0	14.0	14.0

The explanation is that the N of the N-containing Fe leaves the metal and, hence, all the lattice parameters coincide within the error limits.

To check the escape of nitrogen, the lattice parameter of one nitrogen-charged sample was measured below  $780^{\circ}\text{C}$ , at  $760^{\circ}\text{C}$ . Then the sample was heated above  $800^{\circ}\text{C}$  for several hours, cooled down to  $760^{\circ}\text{C}$  and the lattice parameter measured again (the X-ray patterns were on one film). A higher value was now obtained, which can be explained by the escape of nitrogen from the iron.

Fig. 19 shows clearly that small amounts of dissolved N (110 p.p.m.) lower the lattice parameter of Fe at elevated temperatures to such an extent that a straight line relationship in the plot of lattice parameter versus temperature results. Fig. 19 also indicates the reproducibility of the measurements with such samples (the repeated sample F shows a small dip). This behavior of the solid solutions also explains why some iron samples display a distinct Curie point, while others show only a very weak bend if at all. Thus, very easily a straight line can be drawn through all the experimental points (Fig. 19) as it probably was in case of the measurements of Basinski et al., Kim, Dunner et al. and others (see Fig. 8), while Kohlhaas et al. observed a distinct Curie point. Of course, some other impurities in iron may cause a similar

effect.

It follows from those measurements that the inability to observe at times the Curie point by the lattice parameter method is due to the presence of impurities in Fe, of which only the action of nitrogen was explored up to now. Hence, the present results are consistent with the conclusion of Austin and Pierce<sup>(35)</sup>, that small amounts of impurities in iron play an important role in the thermal expansion of this metal at elevated temperature.

## CHAPTER VII

## SUMMARY

1. The lattice parameter of pure nickel at 25°C is:  

$$a = 3.52399 \pm 0.00003 \overset{\circ}{\text{A}}$$
 (with refraction correction)
2. Pure nickel displays a thermal expansion anomaly at the Curie point (350°C). Although the expansivity of nickel is constant in the room temperature range (15-55°C), it increases parabolically with temperature at elevated temperatures, except of an abrupt change in the Curie point region.
3. The lattice parameters of iron at 25°C from one film are:  

$$a = 2.86621 \overset{\circ}{\text{A}}$$
 for 99.999% Fe  

$$a = 2.86624 \overset{\circ}{\text{A}}$$
 for 99.985% Fe  

$$a = 2.86614 \overset{\circ}{\text{A}}$$
 for 99.9% Fe
4. All three grades of iron show a minimum in thermal expansivity at the Curie temperature (770°C) region, having a narrow temperature range of about 30°C. The anomalous change of the thermal expansion is in agreement with the measurements of Ridley and Stuart<sup>(34)</sup> and some earlier workers.
5. The thermal expansion coefficient of pure iron reaches a maximum ( $\alpha=15.9 \times 10^{-6}$  for sample A and  $16.8 \times 10^{-6} \text{ } ^\circ\text{C}^{-1}$

for sample B & sample C) at about  $500^{\circ}\text{C}$ , in agreement with previous results.

6. By employing a very fine powder and a low pressure nitrogen atmosphere, thermal charging ( $600^{\circ}\text{C}$ ) of  $\alpha\text{-Fe}$  with nitrogen is possible. Three samples containing 220, 170 and 110 p.p.m. (within the  $\alpha$ -phase) were obtained and were used for high temperature X-ray work.
7. Nitrogen has no effect (within the limits of errors) on the lattice parameter of iron at room temperature. However, it does depress the thermal expansion of iron at high temperatures, decreasing the lattice parameter of Fe especially in Curie point range.
8. Nitrogen lowers the Curie temperature of iron from  $768^{\circ}\text{C}$  to about  $750^{\circ}\text{C}$  depending on the N content, which agrees with earlier data<sup>(48)</sup>.
9. At a certain nitrogen concentration (110 p.p.m.) in Fe, a bend in the  $a$ - $T$  plot at the Curie temperature can hardly be noticed.
10. Nitrogen escapes from iron at  $780^{\circ}\text{C}$ . Above that temperature the lattice parameters of all the Fe sample investigated agree within limits of error. The "residue"

nitrogen may still cause a slight decrease in the lattice expansion of iron.

## APPENDIX

## DATA AND CALCULATIONS

TABLE XV

Lattice parameter of 99.999% pure iron; sample A  
(For refraction correction add 0.0001 Å)

Film No.	Temperature (°C)	Lattice parameter (Å)
202	18	2.8662
208	18.2	2.8662
206	25	2.8663
255	25	2.8663
208	50	2.8671
231	127	2.8700
231	245	2.8750
223	345	2.8798
225	416	2.8836
224	437	2.8843
231	476	2.8858
224	530	2.8881
231	602	2.8912
214	625	2.8923
214	638	2.8927
214	664	2.8938
215	680	2.8945
216	698	2.8952
217	700	2.8953

TABLE XV -- (continued)

Film No.	$t^{\circ}\text{C}$	$a$ ( $\text{\AA}$ )
215	699	2.8952
206	713	2.8959
205	718	2.8968
206	725	2.8964
207	734	2.8967
217	738	2.8968
221	742	2.8970
207	746	2.8973
221	752	2.8975
208	755	2.8976
208	761	2.8978
209	763	2.8979
209	765	2.8979
210	768	2.8980
210	773	2.8980
202	776	2.8979
220	781	2.8982
210	785	2.8983
210	793	2.8989
211	801	2.8990
211	812	2.8993
221	825	2.8998
212	831	2.9002
212	856	2.9013

---

TABLE XVI

Lattice parameter of 99.985% pure iron; sample B  
(For refraction correction add 0.0001 Å)

Film No.	Temperature (°C)	Lattice parameter (Å)
123	25	2.8663
127	125	2.8704
127	250	2.8755
127	378	2.8814
126	612	2.8916
126	637	2.8926
123	660	2.8938
126	723	2.8964
123	752	2.8975
123	760	2.8978
123	765	2.8978
124	771	2.8979
124	777	2.8980
124	781	2.8981
125	807	2.8993
125	824	2.8999
125	840	2.9006
126	852	2.9014
125	860	2.9015

TABLE XVII

Lattice parameter of 99.9% pure iron; sample C

(For refraction correction add 0.0001 Å)

---

Film No.	Temperature (°C)	Lattice parameter (Å)
67	25	2.8663
68	25	2.8864
69	25.0	2.8863
87	140	2.8709
78	230	2.8745
77	255	2.8755
86	265	2.8760
86	369	2.8806
77	370	2.8806
77	464	2.8848
78	571	2.8892
66	641	2.8930
67	650	2.8934
67	658	2.8937
67	665	2.8940
68	675	2.8943
68	677	2.8944
69	695	2.8952

---

TABLE XVII - (continued)

Film No.	t <sup>o</sup> C	a (Å)
70	700	2.8954
71	711	2.8958
71	723	2.8963
71	728	2.8966
71	738	2.8970
72	745	2.8972
72	750	2.8974
72	754	2.8975
72	756	2.8975
81	763	2.8975
74	767	2.8975
83	773	2.8975
76	783	2.8980
83	794	2.8984
83	802	2.8987
84	821	2.8995
84	840	2.9003
84	859	2.9010
84	879	2.9018
85	892	2.9023
85	900	2.9026

---

---

TABLE XVIII

Lattice parameter of sample D\*\*, containing 220 p.p.m. N

(For refraction correction add 0.0001 Å)

Film No.	Temperature (°C)	Lattice parameter (Å)
510	15	2.8659
512	25	2.8663
510	600	2.8906
518	613	2.8911
510	643	2.8922
518	658	2.8929
514	671	2.8937
510	683	2.8939
517	710	2.8952
514	718	2.8959
518	723	2.8957
517	725	2.8958
515	732	2.8961
518	735	2.8960
512	740	2.8959
511	748	2.8961
511	752	2.8961
519	753	2.8961

TABLE XVIII - (continued)

Film No.	$t^{\circ}\text{C}$	$a$ ( $\text{\AA}$ )
512	768	2.8965
517	772	2.8970
511	773	2.8973
519	778	2.8974
515	780	2.8981
513	785	2.8983
516	795	2.8988
515	820	2.8997
513	827	2.9001
516	842	2.9006
516	858	2.9014
514	877	2.9019

---

---

\*\* See Table X, page 50.

TABLE XIX

Lattice parameter of sample E, containing 170 p.p.m. N

(For refraction correction add 0.0001 Å)

Film No.	Temperature (°C)	Lattice parameter (Å)
610	15	2.8660
605	25	2.8663
602	599	2.8907
602	641	2.8925
606	666	2.8932
602	689	2.8944
602	711	2.8954
608	720	2.8957
601	738	2.8963
603	745	2.8964
609	748	2.8964
608	750	2.8964
603	755	2.8965
603	764	2.8967
603	770	2.8972
609	773	2.8975
605	778	2.8979
604	782	2.8980
604	784	2.8980
604	791	2.8984
607	807	2.8992
606	824	2.8994
605	835	2.9003
607	850	2.9006
604	858	2.9013
607	875	2.9020

TABLE XX

Lattice parameter of sample F, containing 110 p.p.m. N<sub>2</sub>  
 (For refraction correction add 0.0001 Å)

Film No.	Temperature (°C)	Lattice parameter (Å)
850*	612	2.8913
850*	675	2.8937
802	694	2.8948
800	729	2.8960
850*	736	2.8962
800	738	2.8963
850*	742	2.8964
800	742	2.8965
800	752	2.8968
851*	756	2.8968
800	758	2.8970
852*	761	2.8970
801	762	2.8972
801	766	2.8975
852*	767	2.8972
801	772	2.8977
852*	772	2.8977
852*	775	2.8977
801	780	2.8980
801	785	2.8983
852*	787	2.8980
853*	793	2.8983
802	797	2.8988
802	843	2.9004

\* Repeated sample F

Determination of nitrogen in sample D

Using equation (7), page 49,

$$\text{Nitrogen in p.p.m.} = (\text{PVM} \times 1000) / \text{RTW} \times 760$$

where

$$\begin{aligned} P &= 86 \text{ microns} \\ V &= 338 \text{ cm}^3 \\ M &= 28.2 \\ R &= 82.05 \text{ cm}^3\text{-atm/deg. mole} \\ T &= 296.5^\circ\text{K} \\ W &= 0.2 \text{ gram} \end{aligned}$$

Therefore,

$$\begin{aligned} \text{N}_2 \text{ in p.p.m.} &= 86 \times 338 \times 28.2 \times 1000 / 82.05 \times 296.5 \times 0.2 \times 760 \\ &= 221 \text{ (p.p.m.)} \end{aligned}$$

Determination of nitrogen in sample E

Using equation (7), page 49,

$$\text{Nitrogen in p.p.m.} = (\text{PVM} \times 1000) / \text{RTW} \times 760$$

where

$$\begin{aligned} P &= 65 \text{ microns} \\ V &= 338 \text{ cm}^3 \\ M &= 28.2 \\ R &= 82.05 \text{ cm}^3\text{-atm./deg. mole} \\ T &= 296.5 \text{ }^\circ\text{K} \\ W &= 0.2 \text{ gram} \end{aligned}$$

Therefore,

$$\begin{aligned} \text{N}_2 \text{ in p.p.m.} &= 65 \times 338 \times 28.2 \times 1000 / 82.05 \times 296.5 \times 0.2 \times 760 \\ &= 167 \text{ (p.p.m.)} \end{aligned}$$

Determination of nitrogen in sample F

Using equation (7), page 49,

$$\text{Nitrogen in p.p.m.} = (\text{PVM} \times 1000) / \text{RTW} \times 760$$

where

$$\begin{aligned} P &= 42 \text{ microns} \\ V &= 338 \text{ cm}^3 \\ M &= 28.2 \\ R &= 82.05 \\ T &= 296.5 \\ W &= 0.2 \text{ gram} \end{aligned}$$

Therefore,

$$\begin{aligned} \text{N}_2 \text{ in p.p.m.} &= 42 \times 338 \times 28.2 \times 1000 / 82.05 \times 296.5 \times 0.2 \times 760 \\ &= 108 \text{ (p.p.m.)} \end{aligned}$$

## BIBLIOGRAPHY

1. Colby, Phys. Rev. XXX, p506 (1910)
2. Hidnert, Bureau of Standards, Journ. Research, v. p. 1305 (1930)
3. Clarke Williams, Phys. Rev. xl-i, p1011 (1934)
4. W. P. Jesse, Physics, vol.5, no. 6, p147 (1934)
5. E.A. Owen and E.L. Yates, Phil. Mag., S 7, vol.21, no. 142, p809 (1936)
6. R. Kohlhaas, PH. D<sup>u</sup>nner and N. Schmitz-Pranghe, Z. angew. Phys., 23, p245 (1967)
7. P. D<sup>u</sup>nner and R. Kohlhaas, Z. Metallk., 59, p567 (1968)
8. M.E. Straumanis and A. Ievins, " The Precision Determination of Lattice Constants by the Asymmetric Method", Goodyear Atomic Corporation, Portsmouth, Ohio (1959)
9. Me.E. Straumanis and E.Z. AKa, J. Am. Chem. Soc., 73, p5643 (1951)
10. M.E. Straumanis and E.Z. AKa, J. Appl. Phy., 23, p330 (1952)
11. M.E. Straumanis, in Clark: "Encyclopedia of X-rays and Gamma rays", p735, Reinhold Publishing Corp., N.Y. (1963)
12. M.E. Straumanis, Analyt. Chem., 25, p700 (1953)
13. M.E. Straumanis, Am. Mineralog., 37, p48 (1952)
14. S.M. Riad, Ph. D. Thesis, Univ. of Missouri at Rolla (1964)
15. C.D. Kim, Ph. D. Thesis, Univ. of Missouri at Rolla (1966)
16. V.S. Kogan and A.S. Bulatov, Soviet Phys. JETP, vol.5, no. 6, p1041 (1962)
17. B.M. Rovinskii and E.P. Kostyukova, Soviet Phys., Crystallography, 3, 383 (1962)
18. Hull, A.W., Phys. Rev., 10, 661 (1917)
19. Davey, W.P., Phys. Rev., 23, 292 (1924)
20. Blake, F.C., Phys. Rev., 26, 60 (1925)

21. Davey, W.P., *Z. Krist.*, 63, 316 (1926)
22. Mayer, G., *Z. Krist.*, 70, 383 (1929)
23. van Arkel, A.E. & Burgers, W.G., *Z. Metallkunde*, 23, 149 (1931)
24. Bradley, A.J. & Jay, A.H., *Proc. Phys. Soc. (London)*, 44, 563 (1932)
25. Esser, H. & Müller, G., *Arch. Eisenhüttenw.*, 7, 265 (1933)
26. Owen, E.A. & Yates, E.L., *phil. Mag.*, 15, 472 (1933)
27. M.E. Straumanis & A.Z. Ievins, *Z. Physik.*, 98, 461 (1936).
28. Montor., V., *Metallurgia ital.*, 29, 8 (1938)
29. Hanawalt, J.E., Rinn, H.W. & Frevel, L.K., *Ind. Eng. Chem., Anal. Ed.*, 10, 457 (1938)
30. Troiano, A.R. & McGuire, F.T., *Tr. A.S.M.*, 31, 340, (1943)
31. Basinski, A.S., Hume-Rothery, W. & Sutton, A.L., *Proc. Roy. Soc.*, A229, 459 (1955)
32. Goldschmidt, H.J., "Advances in X-ray Analysis", vol.5, 191 (1961)
33. Gorton, A.T., Bitsianes, G. & Joseph, T.L., *Tr. A.I.M.E.*, 233, 1520 (1965)
34. Ridley, N., Stuart, H., *Brit. J. Appl. Phys., Ser. 2*, Vol. 1, 1291 (1968)
35. Austin, J.B. & Pierce, R.H.H., Jr., *Tr. A.S.M.*, 22, 477 (1934)
36. Jette, E.R. & Foote, F., *J. Chem. Phys.*, 3, 605 (1935)
37. Bergen, H., *Ann. Physk.*, 39, 553 (1941)
38. Lu, S.S. & Chang, Y.L., *Proc. Phys. Soc. (London)*, 53, 517 (1941)
39. Thomas, D.E., *J. Sci. Instr.*, 25, 440 (1948)
40. Kochanovska, A., *Physica*, 15, 191 (1949)
41. Swanson, H.E., Fuyat, R.K. & Ugrinic, G.M., *Nat'l. Bureau of Standards Circular*, 539, Vol.IV, 3 (1955)

42. Grønvold, F., Haarlidsen, H. & Vigovde, J., Acta Chem. Scan., 8, 1927 (1954)
43. Owen, E.A. & Williams, G.I., J. Sci. Instr., 31, 49 (1954)
44. Sutton, A.L. & Hume-Rothery, W., Phil. Mag., 46, 1295 (1955)
45. M.E., Straumanis, D.C. Kim, Z. Metallk., 272 (1969)
46. Souder, W. & Hidnert, P., BS. Sci. Pap., 21, 524 (1926)
47. Lehr, P., Compt. rend., 242, 632 (1956)
48. Fry Ad., Stahl und Eisen, 43, 1271 (1923)
49. Pearson, W.B., "A handbook of lattice spacing and structures of metals and alloys", New York, Pergamon Press (1958-67)

## VITA

The author was born on June 23, 1946 in Kaoshiung, Taiwan (Formosa), Rep. of China.

He received his B.S. in Mining & Metallurgical Engineering, June 1968 from the College of Engineering, Provincial (now National) Cheng-Kung University.

After his graduation, he served in the Chinese Army for one year.

He has been enrolled in the Graduate School of the Missouri School of Mines & Metallurgy, since September 1969.